1986-12

Topographic influences in the California current system

Chen, Ching-Yin

NAVAL POSTGRADUATE SCHOOL
Monterey, California

THESIS

TOPOGRAPHIC INFLUENCES
IN THE
CALIFORNIA CURRENT SYSTEM

by

Ching-Yin Chen

December 1986

Thesis Advisor R. L. Haney

SECURITY CLASSIFICATION OF THIS PAGE

REPORT DOCUMENTATION PAGE

1a REPORT SECURITY CLASSIFICATION UNCLASSIFIED	1b. RESTRICTIVE MARKINGS
2a SECURITY CLASSIFICATION AUTHORITY	3 DISTRIBUTION / AVAILABILITY OF REPORT Approved for public release; distribution is unlimited
2b DECLASSIFICATION / DOWNGRADING SCHEDULE	
4 PERFORMING ORGANIZATION REPORT NUMBER(S)	5 MONITORING ORGANIZATION REPORT NUMBER(S)
6a. NAME OF PERFORMING ORGANIZATION Naval Postgraduate School 6b OFFICE SYMBOL (*If applicable*) Code 68	7a. NAME OF MONITORING ORGANIZATION Naval Postgraduate School
6c. ADDRESS (*City, State, and ZIP Code*) Monterey, California 93943-5000	7b. ADDRESS (*City, State, and ZIP Code*) Monterey, California 93943-5000
8a NAME OF FUNDING / SPONSORING ORGANIZATION 8b. OFFICE SYMBOL (*If applicable*)	9. PROCUREMENT INSTRUMENT IDENTIFICATION NUMBER
8c. ADDRESS (*City, State, and ZIP Code*)	10 SOURCE OF FUNDING NUMBERS PROGRAM ELEMENT NO / PROJECT NO / TASK NO / WORK UNIT ACCESSION NO

11 TITLE (*Include Security Classification*)
TOPOGRAPHIC INFLUENCES IN THE CALIFORNIA CURRENT SYSTEM

12 PERSONAL AUTHOR(S)
Chen, Ching-Yin

13a TYPE OF REPORT	13b TIME COVERED	14 DATE OF REPORT (*Year, Month, Day*)	15 PAGE COUNT
Master's Thesis	FROM _____ TO _____	1986 December	50

16 SUPPLEMENTARY NOTATION

17 COSATI CODES			18. SUBJECT TERMS (*Continue on reverse if necessary and identify by block number*)
FIELD	GROUP	SUB-GROUP	topography, instability, barotropic, baroclinic, slope, escarpment, stable, unstable, numerical, CCS, bottom, jet, coast, along-shore, flow.

19 ABSTRACT A ten-level primitive equation numerical model is used to study the influences of the bottom topography in the California Current System. Five different numerical experiments were integrated for 40 days after being initialized with a baroclinic along-shore coastal jet representative of the observed coastal jet. By comparison with a flat bottom case, in Experiments 1 and 3, in which the topographic slopes face westward or northward, the topography appears to have stabilizing influences on the mean flow. In Experiments 2 and 4, in which the topographic slopes face southward, the topographic β-effect appears to be strong enough so that these two cases have already reached a quasi-steady state by 40 days. This is because in Experiments 2 and 4 the long, non-dispersive topographic Rossby waves are effective at transporting the eddy energy away from the source region near the coast. The resulting new mean flow appears to be stable.

20 DISTRIBUTION / AVAILABILITY OF ABSTRACT	21. ABSTRACT SECURITY CLASSIFICATION
☒ UNCLASSIFIED/UNLIMITED ☐ SAME AS RPT ☐ DTIC USERS	unclassified
22a NAME OF RESPONSIBLE INDIVIDUAL R. L. Haney	22b TELEPHONE (*Include Area Code*) (408) 646-2308 22c OFFICE SYMBOL 63Hy

DD FORM 1473, 84 MAR 83 APR edition may be used until exhausted
All other editions are obsolete

SECURITY CLASSIFICATION OF THIS PAGE

Approved for public release; distribution is unlimited.

Topographic Influences in The California Current System

by

Ching-Yin Chen
Lieutenant Commander, Republic of China
B.S., Chinese Naval Acadamy, 1976

Submitted in partial fulfillment of the
requirements for the degree of

MASTER OF SCIENCE IN OCEANOGRAPHY

from the

NAVAL POSTGRADUATE SCHOOL
December 1986

ABSTRACT

A ten-level primitive equation numerical model is used to study the influences of the bottom topography in the California Current System. Five different numerical experiments were integrated for 40 days after being initialized with a baroclinic alongshore coastal jet representative of the observed coastal jet. By comparison with a flat bottom case, in Experiments 1 and 3, in which the topographic slopes face westward or northward, the topography appears to have stabilizing influences on the mean flow. In Experiments 2 and 4, in which the topographic slopes face southward, the topographic β-effect appears to be strong enough so that these two cases have already reached a quasi-steady state by 40 days. This is because in Experiments 2 and 4 the long, nondispersive topographic Rossby waves are effective at transporting the eddy energy away from the source region near the coast. The resulting new mean flow appears to be stable.

TABLE OF CONTENTS

LIST OF TABLES

LIST OF FIGURES

I. INTRODUCTION

The eastern boundary current regime off the coast of California is characterized by the development and evolution of eddy activity and by a continual interaction between this eddy activity, the "mean" California Current System (CCS), and important physical processes in the mixed layer. Baroclinic instability of the seasonal mean flow has been identified as an important generating mechanism in the Northeast Pacific Ocean, and off Vancouver Island (Wright, 1980; Emery and Mysak, 1980; Thomson, 1984). It has also been shown to be important off the coast of Northern California and Orgeon (Ikeda and Emery, 1984), and it may also be an important mechanism in the central California coast region as well. The pronounced mesoscale eddy activity in the CCS has been identified and best seen in satellite IR images, especially those from the AVHRR on board NOAA-6. An eddy seen in such satellite data during the CODE experiment off Vancouver Island (Thomson, 1984) was shown to develop due to baroclinic instability and it was observed (in CTD and XBT data) to extend form the surface to a depth of 1 km. In the CCS however, the vertical structure of the eddies is not well known. Furthermore, the kinematics, the energetics and the vertical structure of an eddy may change with time as the eddy evolves and migrates off-shore and downstream into the "mean" CCS.

In most studies of flow over topography, it has been found that the slope effect (topographic-β) acts to stabilize the flow. However there are two recent studies of flow over topography which indicate that enhanced instability can result. The first study is the analytic work of Charney and Flierl (1981), who demonstrated that the stability of a parallel mean flow in the presence of topography can be quite different from that of the identical mean flow in a flat bottomed ocean. They examined the specific problem of destabilization of the mean flow by form drag instability of a baroclinic flow which is neutrally stable in the absence of topography. The instability occurs for topographic scales of the order of 70-100 km, with growth rates proportional to the topographic height. This means that the available potential energy of the mean flow can be trapped by the orographic instability even in situations where normal baroclinic instability is unable to extract energy from the mean flow. The second study is laboratory modeling by Narimousa and Maxworthy (1985). In their experiments, coastal upwelling is

produced by an along-shore stress in a rotating cylindrical tank in the presence of a cone-shape ridge in the bottom topography. As the upwelling process continues, the interface (front) between the two layers of the two-layer fluid used in the tank surfaces and moves away from the wall (coast). When the front has reached a certain distance from the wall, baroclinic waves develop on the front, and large standing waves develop downstream of the topographic ridge. Under some circumstances, cyclones pinch off, both from the upstream front at the topographic ridge and from the crests of the large standing waves downstream of the ridge. These laboratory results show many features reminiscent of eddy flows recently observed in the CCS. The results of these investigations suggest that a study of the baroclinic and barotropic instability processes over a pronounced escarpment normal to the coast is needed to fully understand the oceanic eddy field off the coast of central California.

This study is designed to identity the role of topography in modifying the stability of the CCS. An objective is to determine whether the eddy field in the CCS is the result of an instability of the mean flow or not, and whether the topography effects the instability. This is done by performing initial value numerical experiments with an existing multi-level primitive equation model adapted to the CCS. The model domain covers 6° longitude by 6° latitude and has approximately 8 km × 10 km horizontal resolution with 10 levels in vertical. The space staggered B-scheme in horizontal and a σ coordinate system in vertical were used. Five different numerical experiments with four different bottom topographies and one flat bottom case were performed. We note that the results of the experiments were different and in the results have different interpretations.

II. MODEL AND EXPERIMENTS DESIGN

A. MODEL DESCRIPTION

The purpose of this study is to investigate the influences of the topography in the CCS. The present numerical experiment uses a ten level primitive equation model (Haney, 1985). The model is in sigma coordinates (non-dimentional depth) and has open boundaries (Camerlengo and O'Brien, 1980) on all but the eastern coastal boundary.

The present domain of the model ocean is the rectangular region extending from approximately 124° W to 130° W and from 36.5° N to 42.5° N (Fig 2.1). The present model has 65 × 65 = 4225 grid points uniformly spaced in the horizontal with a resulting grid spacing of 8 km in the east-west direction and 10 km in the north-south direction. Figs. 2.2-2.6 show 3-dimensional perspective plots of the actual bottom topography of the region and those used in the model ocean. Four numerical experiments, each with a different bottom topography (Figs. 2.3-2.6), were run in order to study the role an idealized escarpment (Mendoceno Escarpment) on the CCS.

This study only focuses on the influences of variable bottom topography, because a variable bottom topography may be a more important factor than an irrgular coastline (Peffley and O'Brien, 1976; Preller and O'Brien, 1980). This conclusion is also supported by the recent and highly relevant laboratary modeling work by Narimousa and Maxworthy (1985). In the four experiments there was no wind or thermal forcing, but the initial temperature field was specified so as to produce a geostophically balanced, meridional (long-shore) shear flow having a gaussian-shaped jet. The model is based on the primitive equations which are integrated in time starting from the specified initial condition.

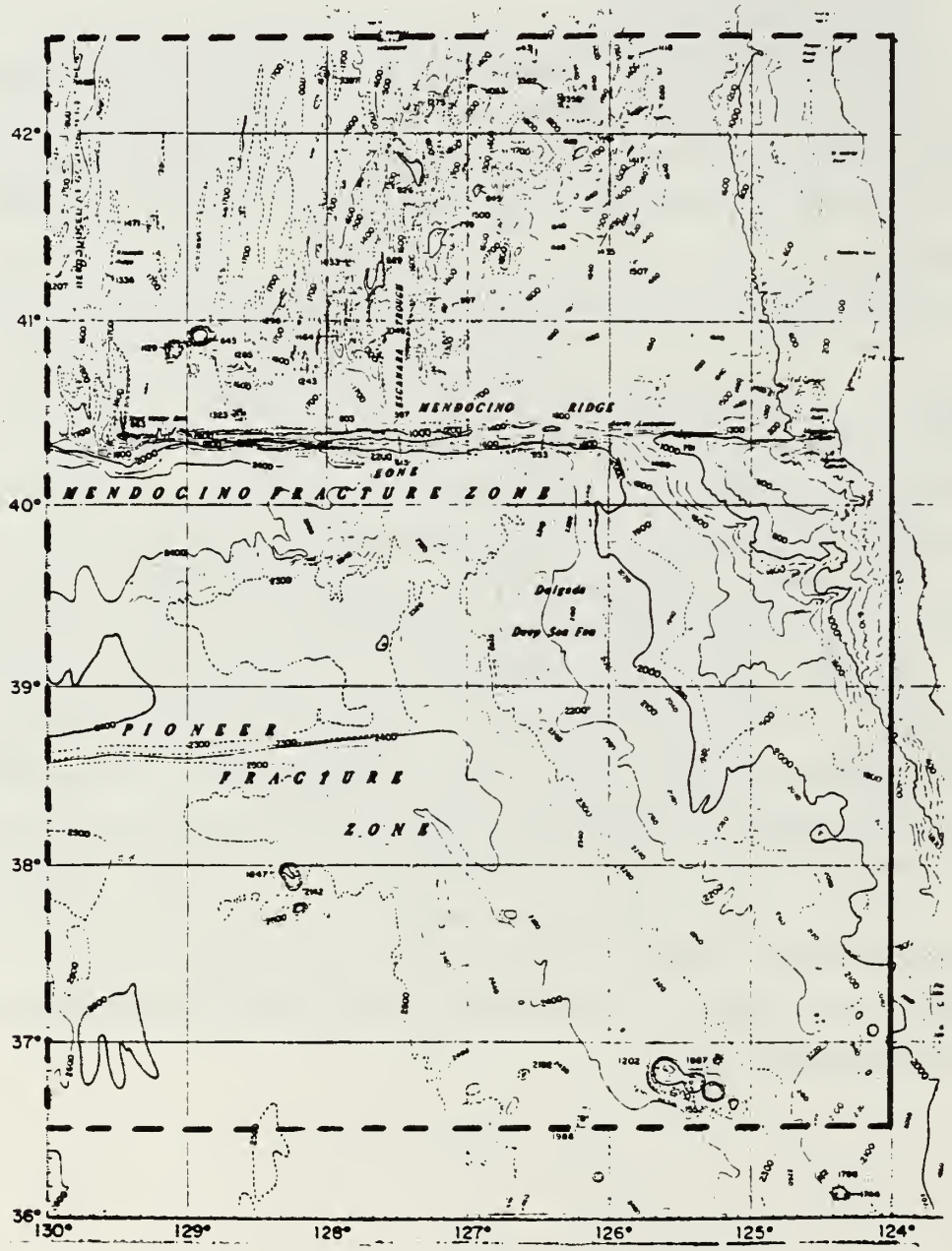

Figure 2.1 Model region.

B. EXPERIMENTS DESIGN

The numerical model was used in this study to carry out four different topographic experiments:

1. off-shore slope only
2. escarpment with shallowest depths to the north
3. escarpment with deepest depths to the north
4. ridge

Of these configurations, Fig. 2.3 corresponds to the continental rise off California, Fig. 2.4 corresponds to an idealized Mendoceno Escarpment, while Fig. 2.5 and Fig. 2.6 are for comparison with Fig. 2.3 and Fig. 2.4. The laboratory experiments of Narimousa and Maxworthy (1985) used a ridge (Fig. 2.6), but an escarpment (Fig. 2.4) is clearly more realistic of the actual topography in the CCS.

The initial temperature field approximately followed the Orlanski and Cox (1973) paper, which was a study of the Gulf Stream, but modified to represent the CCS. In order to define a baroclinic jet corresponding to the CCS, and to fit the OPTOMA (Whittman, et al, 1985) profile of buoyancy frequency N^2 (largest N^2 at about depth 100m) and temperature in the upper ocean, we used four analytic expressions for temperature. In addition, we disturbed the equilibrium state with a small random pertubation in the temperature field. The random number (R) was between -0.05 and +0.05 °C, and it was made to decrease in magnitude with increasing depth. We need larger surface temperature gradients because there is no wind forcing in this model. The realistic surface temperature is 10°C in-shore and 18°C off-shore in summer, so we have to adjust T_x and T_z, to get both a realistic surface temperature and geostrophic transport as in Freitag and Halpern (1981). In addition, we use T_3 and T_4 to fit the N^2 profile in the OPTOMA data. So the analytic expression for the initial temperature is defined as follows:

$$T = T_0 + T_x \times T_z + T_3 + T_4 + R \times \exp(-zzz/450.) \qquad \text{(eqn 2.1)}$$

$$T_0 = TBOT = 2.°C$$

$$T_x = 3 - (\varepsilon x + 1)\exp(-\varepsilon x) \times DT$$

$$T_z = \exp(-zzz/150.)$$

$$T_3 = AMP1 \times (-zzz/L + 1 + 1/2\pi(\sin(2\pi(1/2 - zzz/L)))), \text{ for zzz less than L}$$

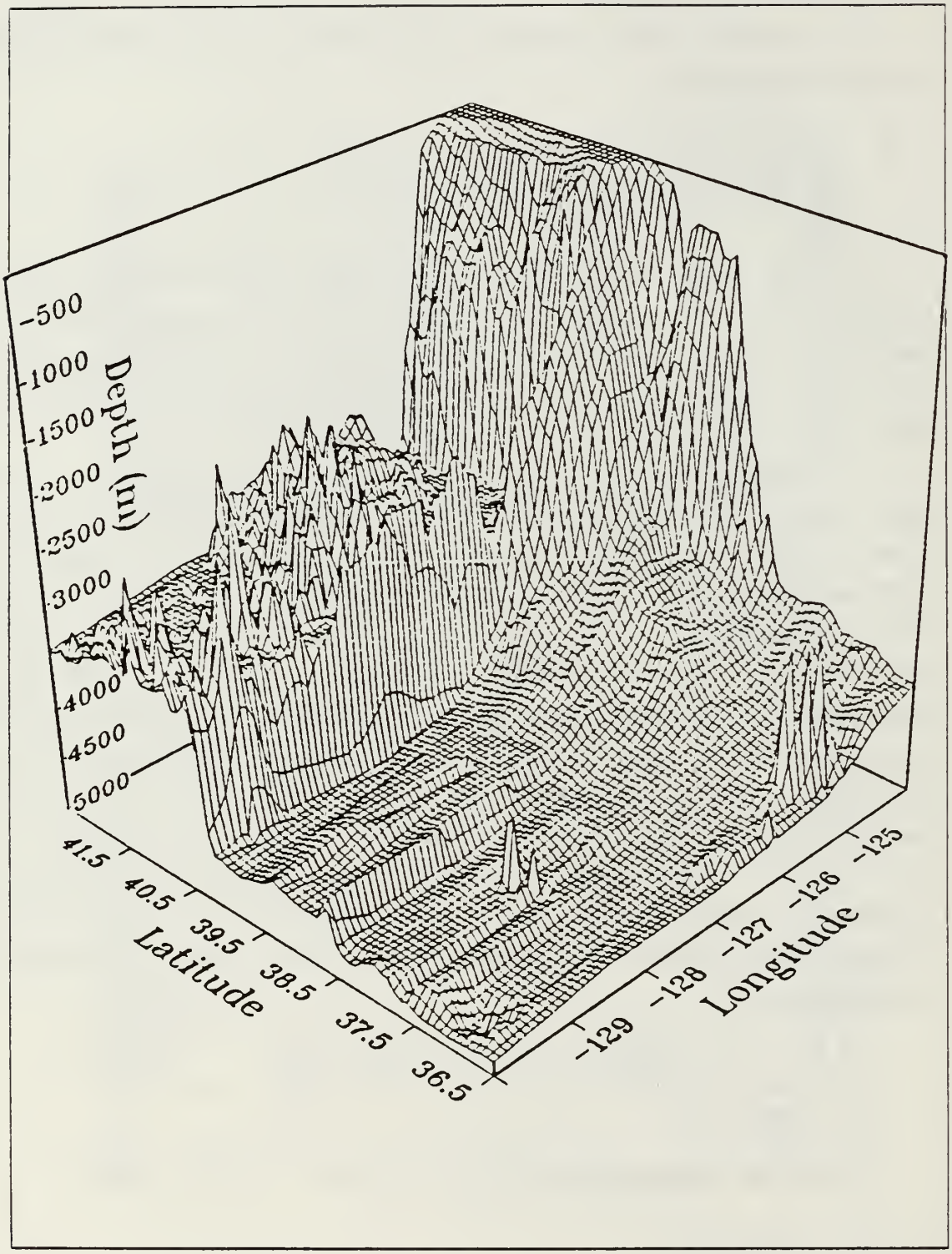

Figure 2.2 Actual bottom topography.

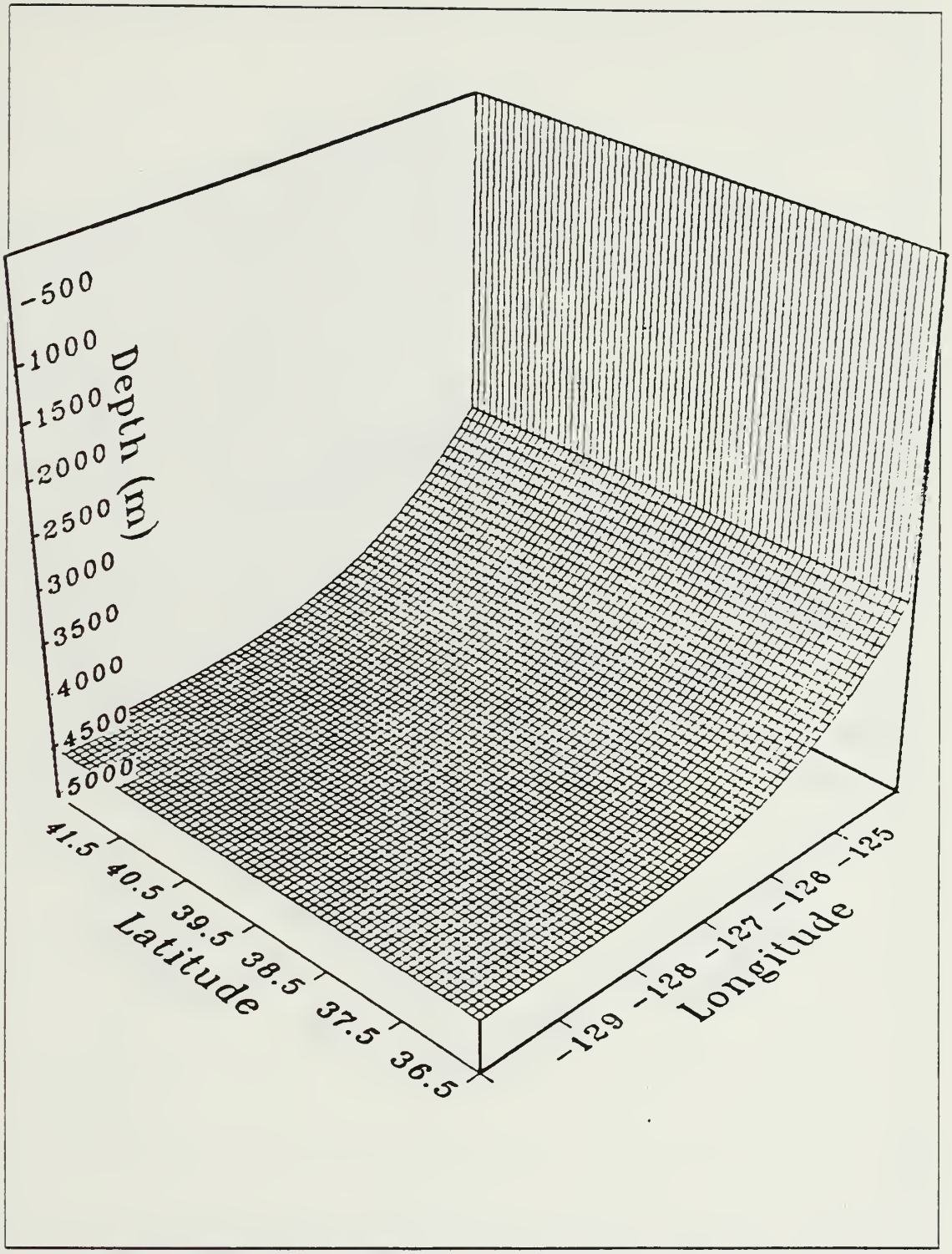

Figure 2.3 Off-shore slope only.

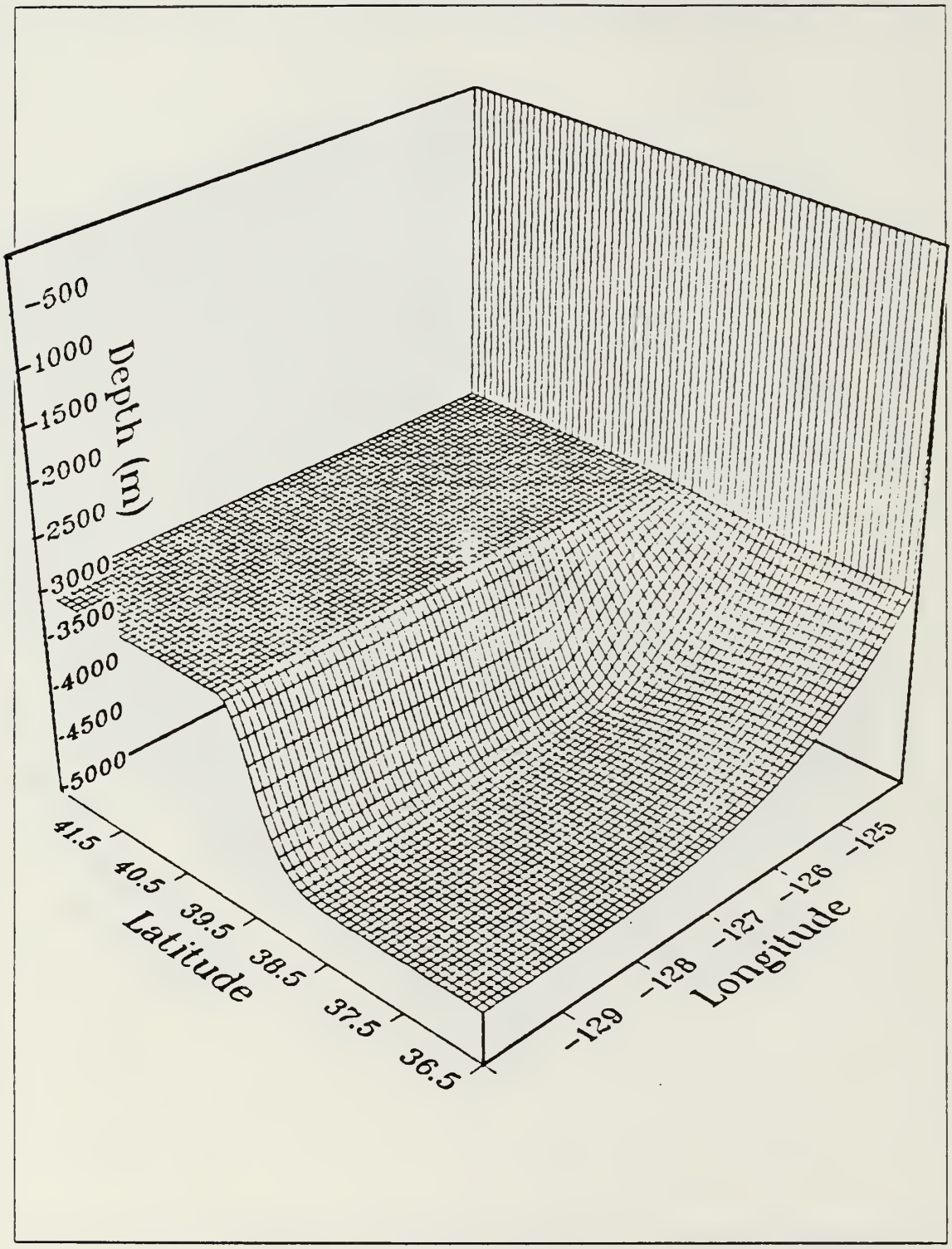

Figure 2.4 Escarpment with shallowest depths to the north.

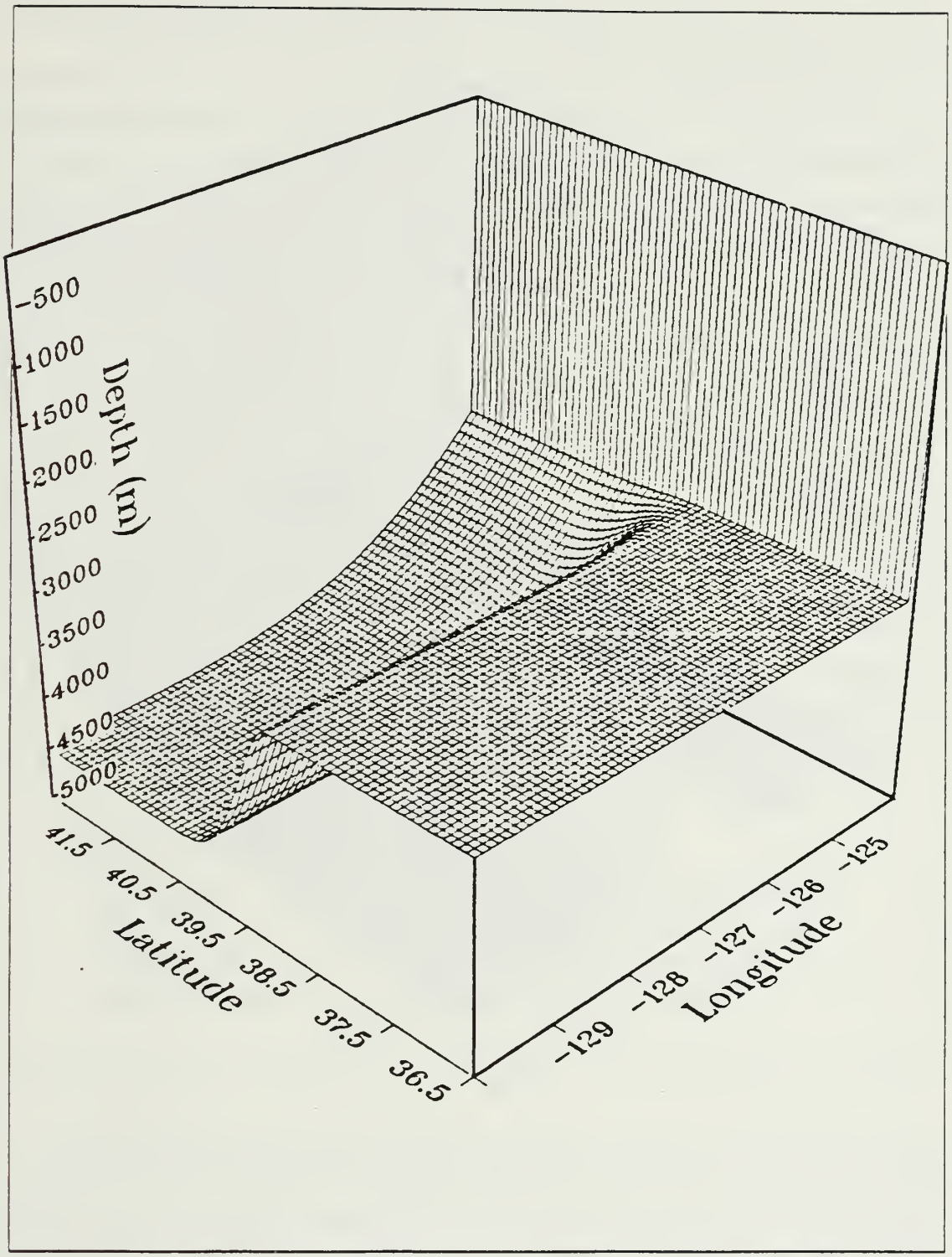

Figure 2.5 Escarpment with deepest depths to the north.

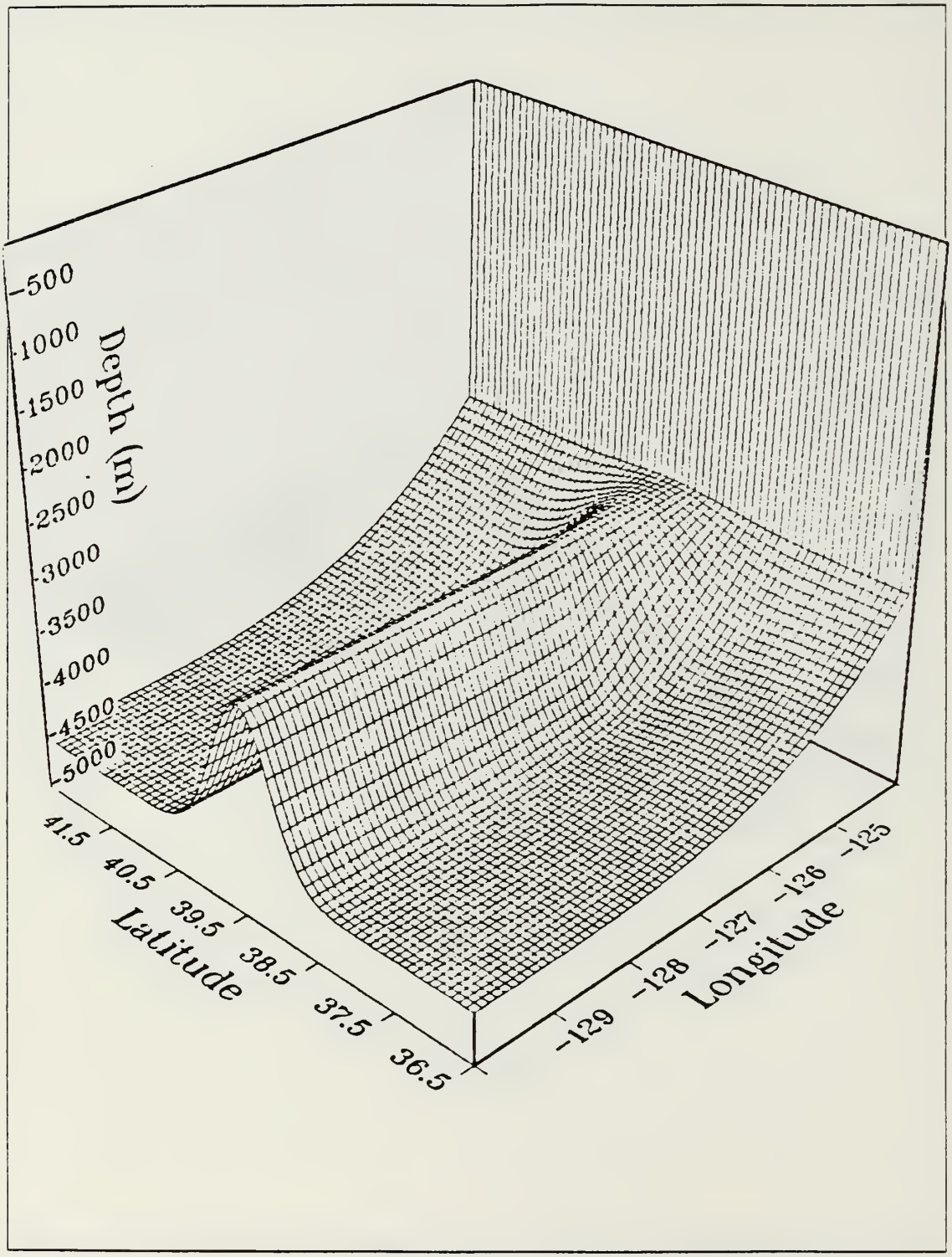

Figure 2.6 Ridge.

T_4 = AMP2 × exp (-zzz/450.)

In these expressions x is distance off-shore, zzz is depth (in meters, positive downward) and $1/\varepsilon$ is the off-shore length scale for the baroclinic jet (40 km). The vertical scale for the jet is 150 m and the vertical scale for the main thermocline (and the random disturbance) is 450m. T_x is defined so as to produce a realistic alongshore geostrophic baroclinic jet,V(x,z). This is done using the hydrostatic and geostrophic (thermal wind) relation and the assumption that the vertical average current is zero.

The constants used in this model are in Table 1.

TABLE 1
VALUES OF CONSTANT USED IN THE MODEL

DTAU = 800. sec	integration time step
G = 981.0 cm/sec^2	acceleration of gravity
C_p = 0.958 cal/(gm ∘K)	specific heat of sea water
T = 273.2 ∘K	reference temperature
α = 2.0 × 1.0E-4 (1/∘k)	thermal expansion coefficient
F = 1.0E-4 (1/sec)	coriolis parameter
Ω = 2π/day	earth rotation rate
ρ = 1.0276 gm/cm^3	density
D00 = 4500m	deepest ocean depth
L = 200m	wavelength for the seasonal thermocline
DT = 11∘C	horizontal temperature variation
AMP1 ~ 3∘C	amplitude of seasonal thermocline
AMP2 ~ 12∘C	amplitude of main thermocline

Since the slopes of the bottom topographies used in the experiments (Figs. 2.3-2.6) are not excessive, the resulting model flows can be interpreted (at least qualitatively) using quasi-geostrophic theory. From the quasi-geostophic potential vorticity equation we can define two parameters γ and δ which describe the potential for mean flow instibilities (Killworth, 1980). The parameter γ is the ratio of the

horizontal length scale of the jet to the Rossby radius of deformation, and δ is the ratio of layer depths (or the fraction of the water column that has $N^2 \neq 0$).

Killworth (1980) showed that the character of the instability (if any) is determined by the behavior of the quantity $\gamma^2\delta^2\partial/\partial z(V_z/N^2)$. This quantity computed from the initial temperature field changes smoothly by 3 to 4 orders of magnitude from the sea surface to the bottom. Since the vertical scale for V is smaller than the vertical scale for T, this term approaches zero at great depth. This type of behavior for this term means that mixed (barotropic / baroclinic) instability is possible in the upper ocean layers, but only barotropic instability is possible at great depth.

We tried three different experiments to determine the optimal placing of the ten model sigma levels. Firstly, the original model sigma levels which included wind forcing, had finer resolution in the upper ocean than lower ocean. Secondly, ten equal spaced sigma levels which gives relatively poorer vertical resolution in the upper ocean were tried. Thirdly, we choose a distribution of levels which has good vertical resolution of $\partial/\partial z(V_z/N^2)$ throughout the water column because the study focuses on the influences of topography. The final decision for the sigma levels is shown in Table 2.

TABLE 2
TABLE OF SIGMA LEVELS

sigma	.01	.035	.075	.135	.215
depth(m)	22.5	101.3	247.5	472.5	787.5
sigma	.315	.441	.597	.783	1.
depth(m)	1192.5	1701.0	2335.5	3105.0	4011.7

A plot of the cross section of the initial baroclinic velocity field used in the four experiments (computed from the eqn 2.1 using the thermal wind equation) is shown in Fig.2.7. The strongest velocity at the surface is 40 cm/sec (southward) at 40 km off-shore and zero velocity at depth 720m. This particular southward jet is representative of the observed CCS coastal jet in the spring and early summer, having been spun up

by upwelling-favorable winds (Kosro and Huyer, 1986). Its transport, which is 5.1 Sv, is also representative of observations (Freitag and Halpern, 1981). The temperature field is shown in Fig. 2.8. The surface temperature is 7.5∘C at the coast and 17.5∘C off-shore which are also representative of summer observations. The potential vorticity is shown in Fig. 2.9. The potential vorticity was computed from the model temperature and currents using the expression from Holton, 1981, page 92. In Fig. 2.9 the potential vorticity is positive except near shore above 150m. The horizontal gradient of potential vorticity is shown in Fig. 2.10. Since the horizontal gradient changes sign in the domain, instability of the jet is possible. However,since the gradient of potential vorticity in the upper ocean is everywhere negative, the horizontal shear will probably serve as a stabilizing (β-type) effect.

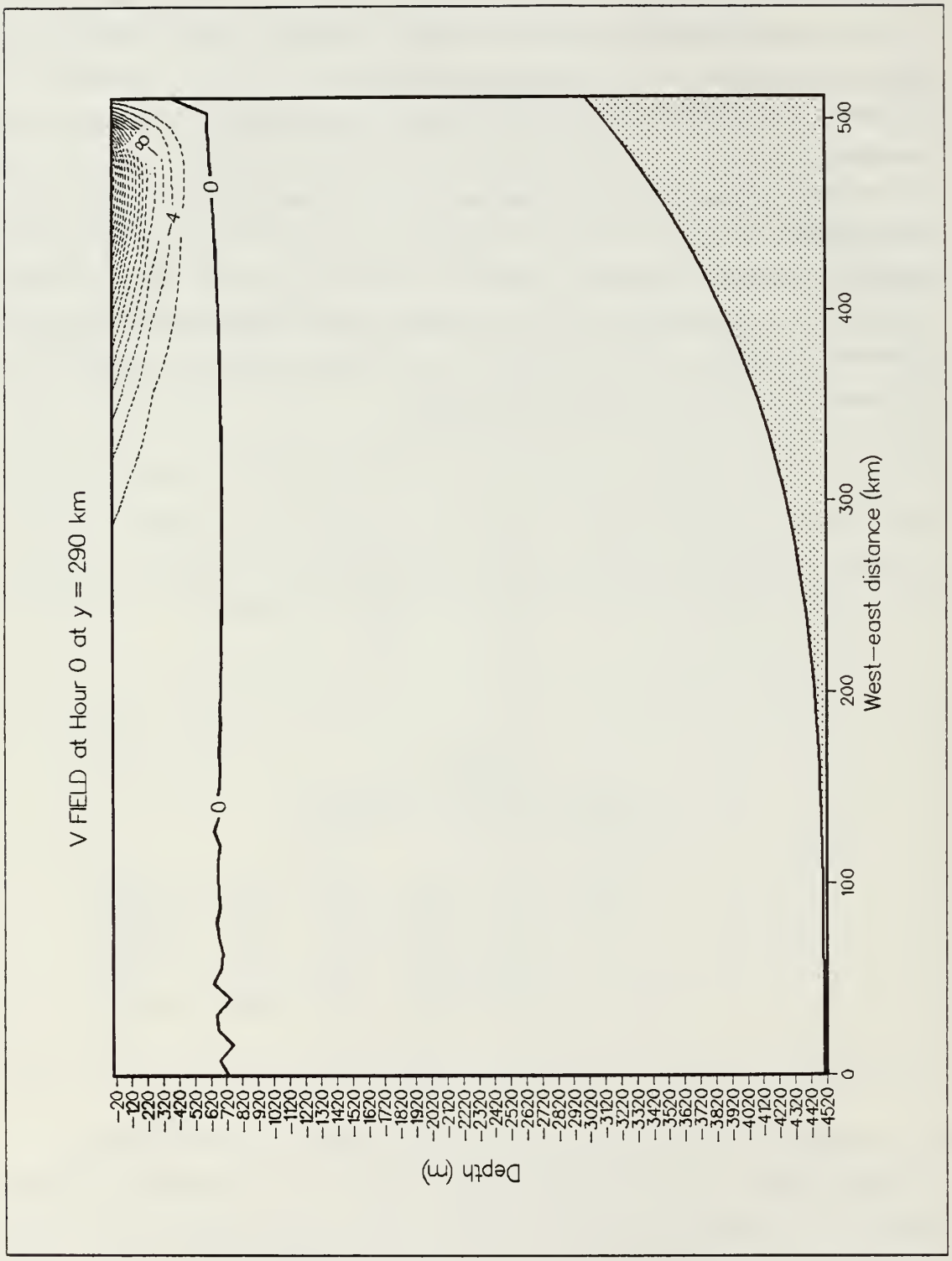

Figure 2.7 Velocity field with contour interval 2 cm/sec.

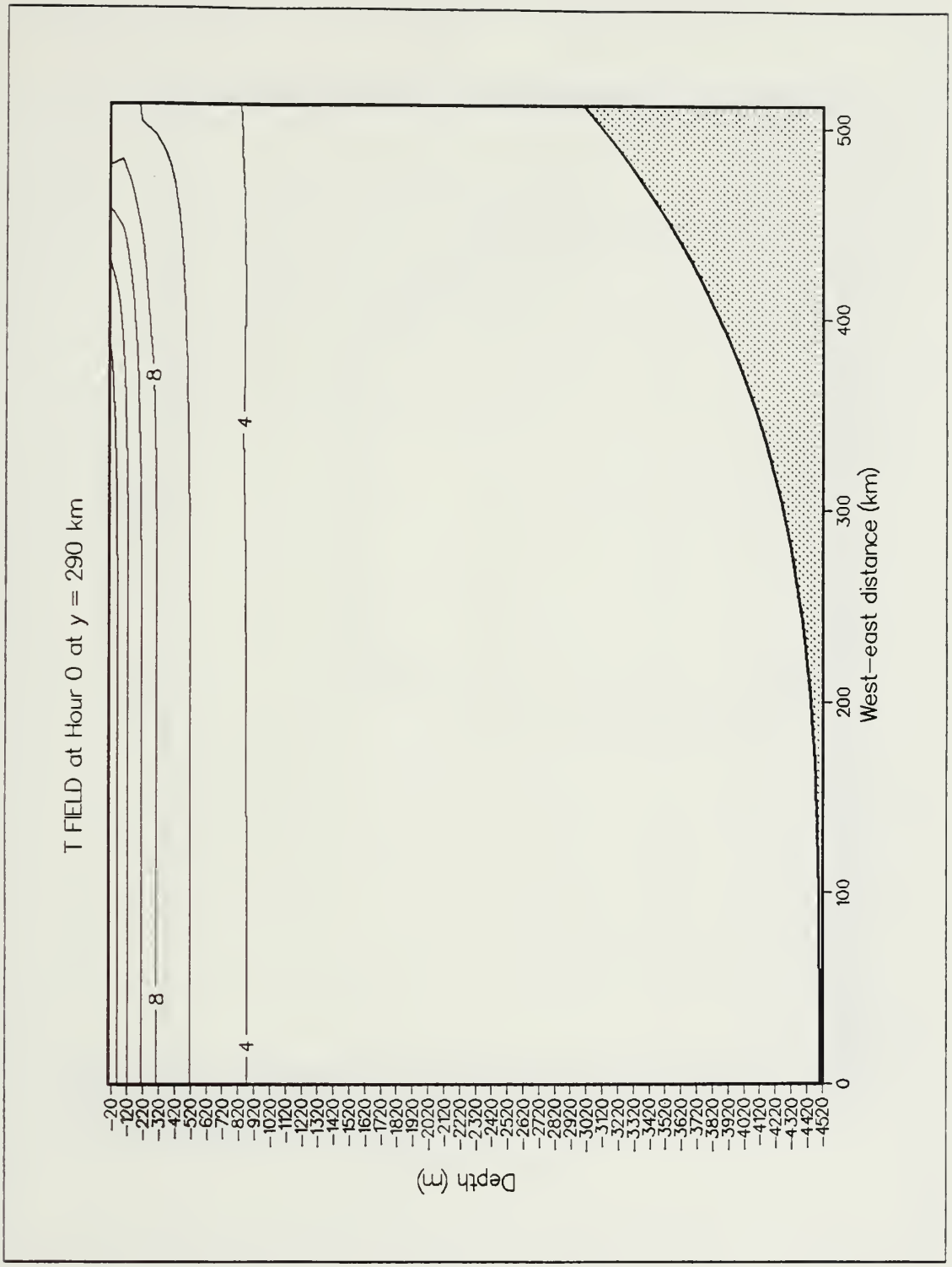

Figure 2.8 Temperature field (∘C, with contour interval 2 ∘C).

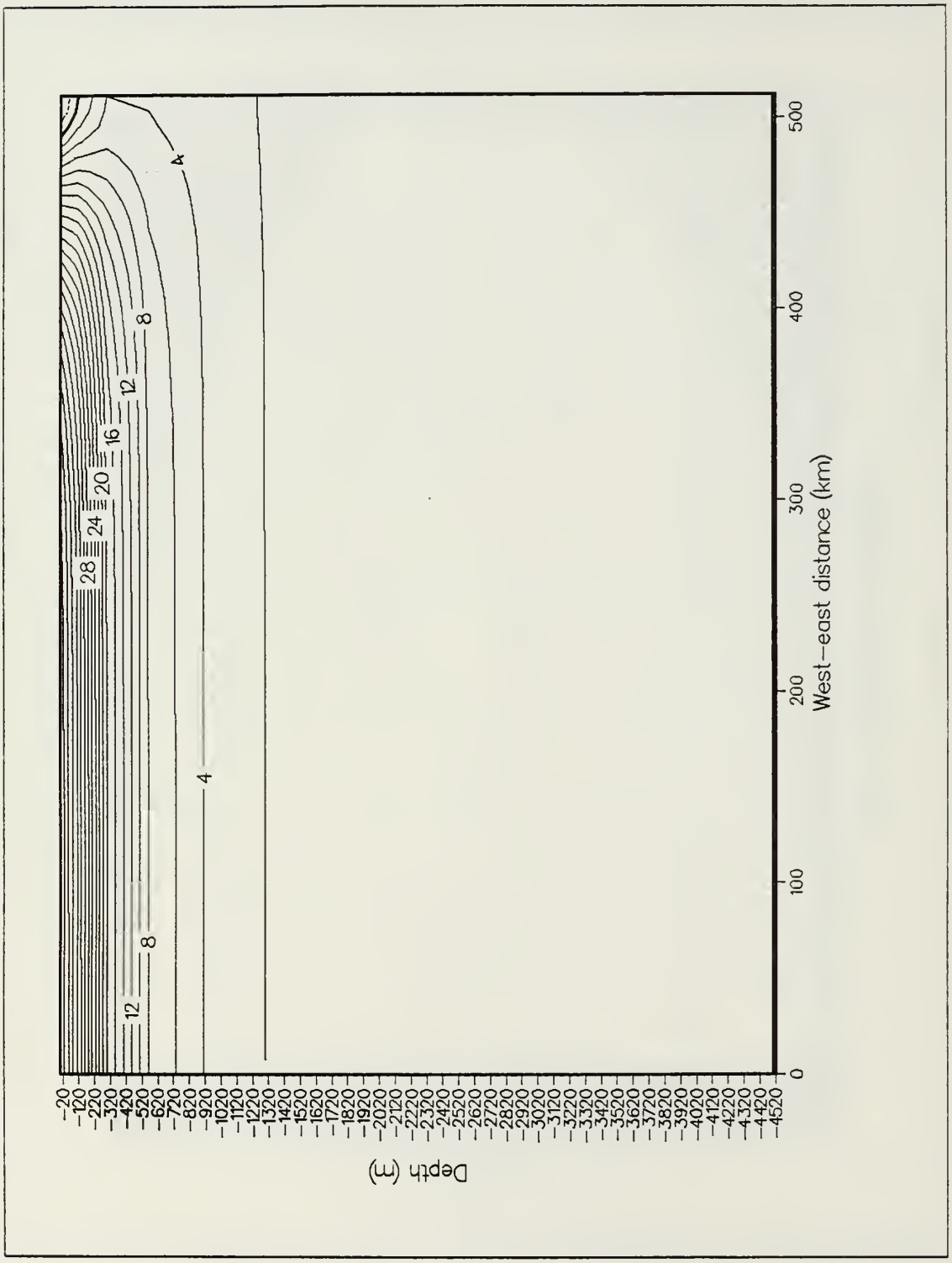

Figure 2.9 Potential vorticity ($1/(sec^2 cm)$).

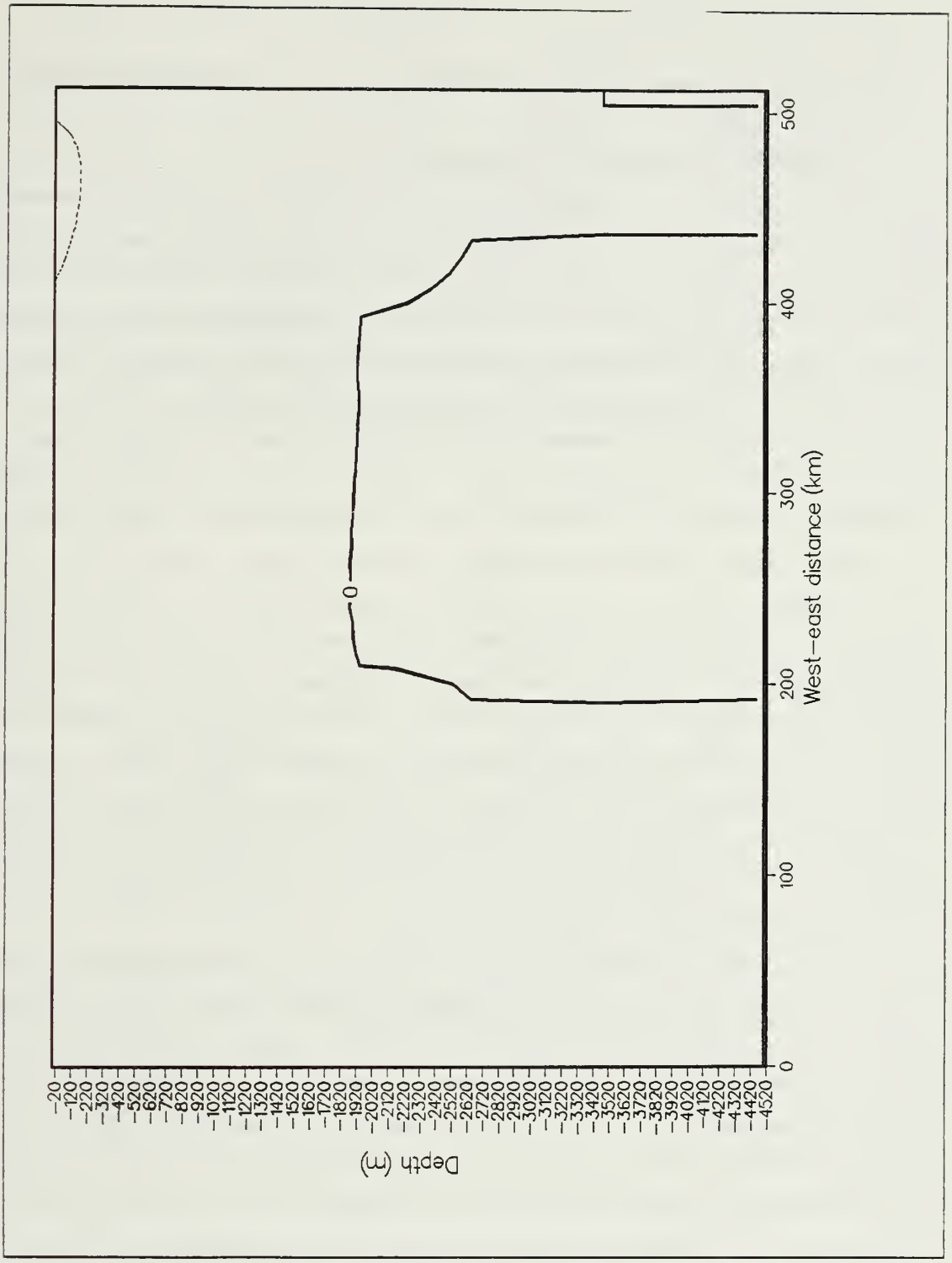

Figure 2.10 Gradient of potential vorticity ($1/(sec^2cm^2)$).

III. RESULTS AND ANALYSIS OF NUMERICAL EXPERIMENTS

A. EXPERIMENT 1 (OFF-SHORE SLOPE ONLY)

The first experiment considers the response of flow over an off-shore topographic slope which has the continental rise depth at the coast of 3000 m and the deepest ocean depth of 4500 m (Fig. 2.3). In this case the maximum surface velocity is 40 cm/sec southward. The experiment of the flow over the topography neglects the depth average velocity component. Only the baroclinic flow over the topography is studied. The effect of this approximation will be examined in future studies.

The experiment was integrated to 40 days to determine the response of the flow to the topography. The resulting surface U-field (eastward, or on-shore velocity component), developed in a time series (every two days) is shown in Fig. 3.1 and Fig. 3.2. The plot shows only the eastern half of the model domain, within 256 km of the eastern boundary. There are only small waves during the first ten days and they are entirely due to the initial random temperature disturbance. The disturbances propagate southward at about 14 cm/sec. The dominant wavelength increases with time from about 50 km at 18 days to 130 km at 30 days. There are only small amplitude waves north of 380 km. The eddies become stronger with time as they propagate southward (spatial and temporal growth). The eddy velocity decreases with increasing depth, and is very weak below 1000 m (not shown). During the entire experiment, the growing disturbances were tilted (in the (x,y) plane) in the direction of the mean jet, a tilt associated with barotropic damping of the eddies.

Fig. 3.3 shows four different fields at 40 days. The in-shore temperature is 9°C and off-shore temperature is 18°C. The temperature field is affected by the geostrophic velocity which is determined by the pressure field. There is a strong baroclinic disturbance near y = 192 km, whose isotherm pattern has been distorted into a kind of "cold front", propagating southward. The growth of this disturbance must be due to baroclinic instability because, as noted above, the trough axis tilts in such a way that eddy V-momentum converges into the mean southward flow. The pressure field at 40 days at depth 125 m (not shown) and surface are in phase, indicating that most of the baroclinic development is about ended.

A flat bottom case was integrated to 40 days to determine (by comparison with Experiment 1) the response of the flow to the topography alone. Fig. 3.4 shows the same four different fields for the flat bottom case at 40 days. By comparing the flat bottom case and Experiment 1 we can see that the flat bottom case has stronger eddy velocities than Experiment 1. In fact, the eddy velocities in Experiment 1 at day 32 were about the same as those in the flat bottom case at day 22. Thus the continental rise topography has a stabilizing influence on the mean flow, so the flat bottom case goes unstable approximately ten days earlier than Experiment 1. As shown below (subsection E), the stabilizing effect is due to the topographic β-effect. This effect can be seen by the fact that the eddies in the flat bottom case do not tilt in the direction of the mean flow as much as the eddies in the topographic case.

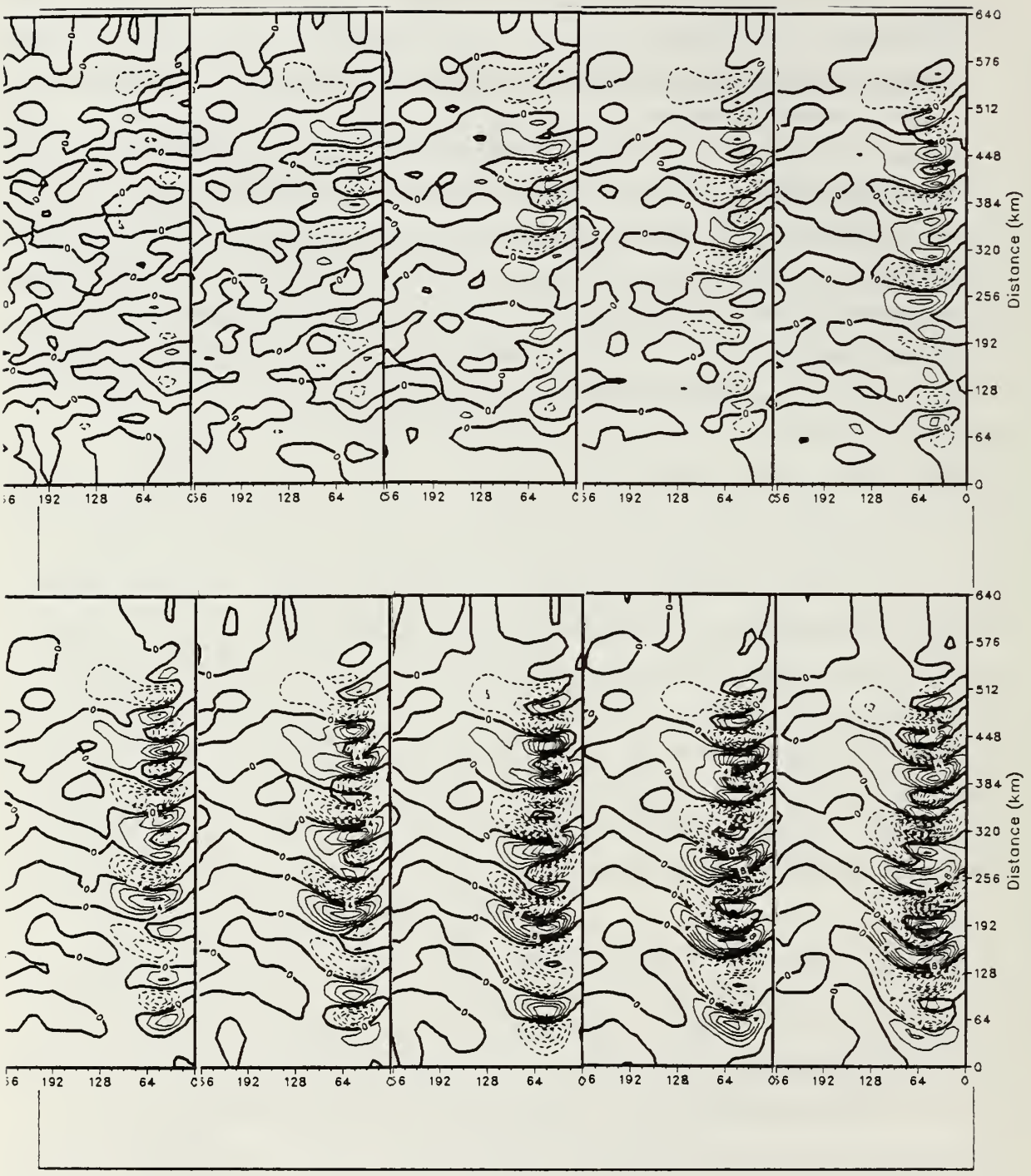

Figure 3.1 U-field in Experiment 1 from 2-20 days in time series (every 2 days), with contour interval 2 cm/sec..

Dashed lines show negative values and indicate off-shore flow, while solid lines show positive values and indicate on-shore flow.

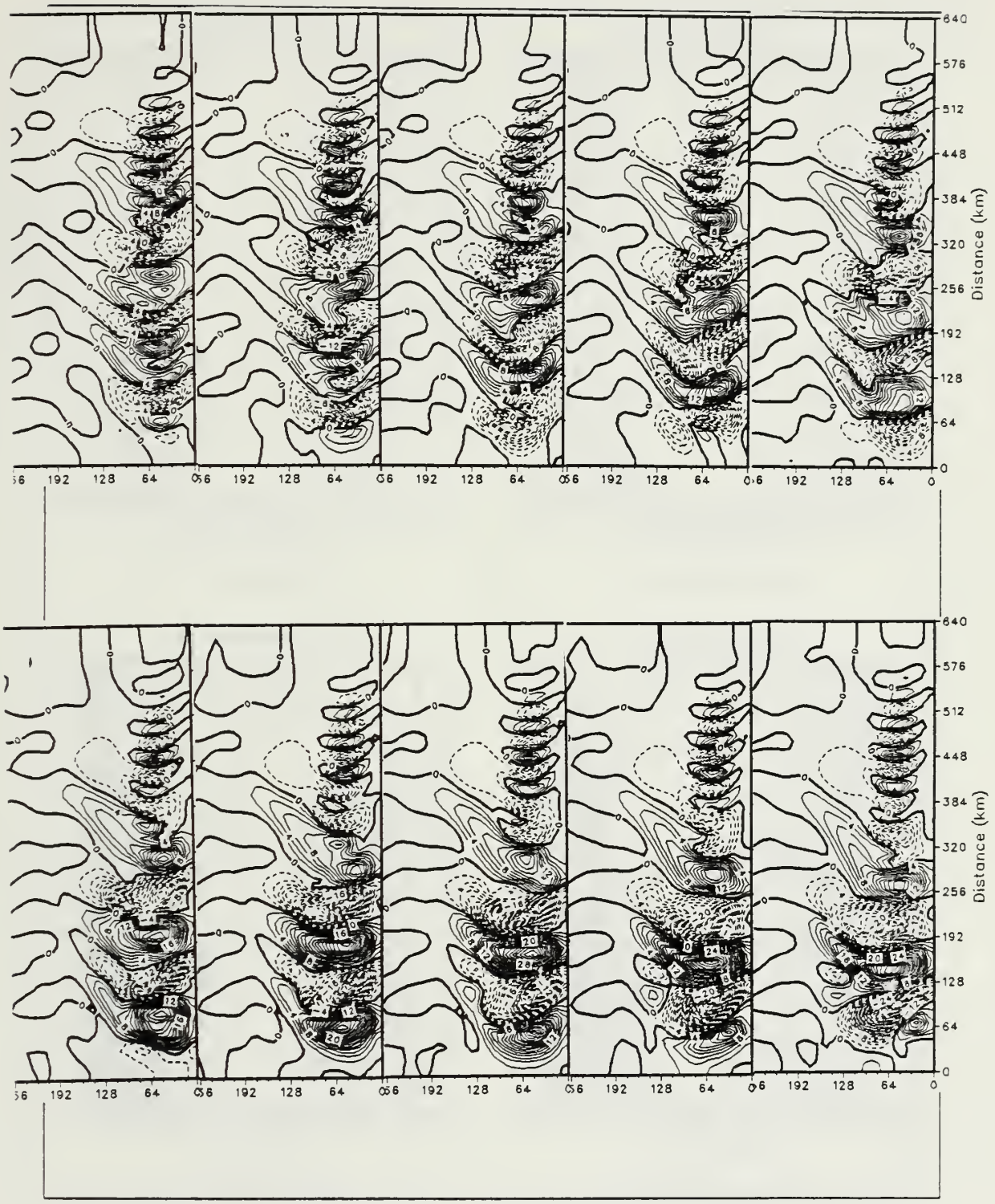

Figure 3.2 The same as Fig. 3.1 except 22-40 days.

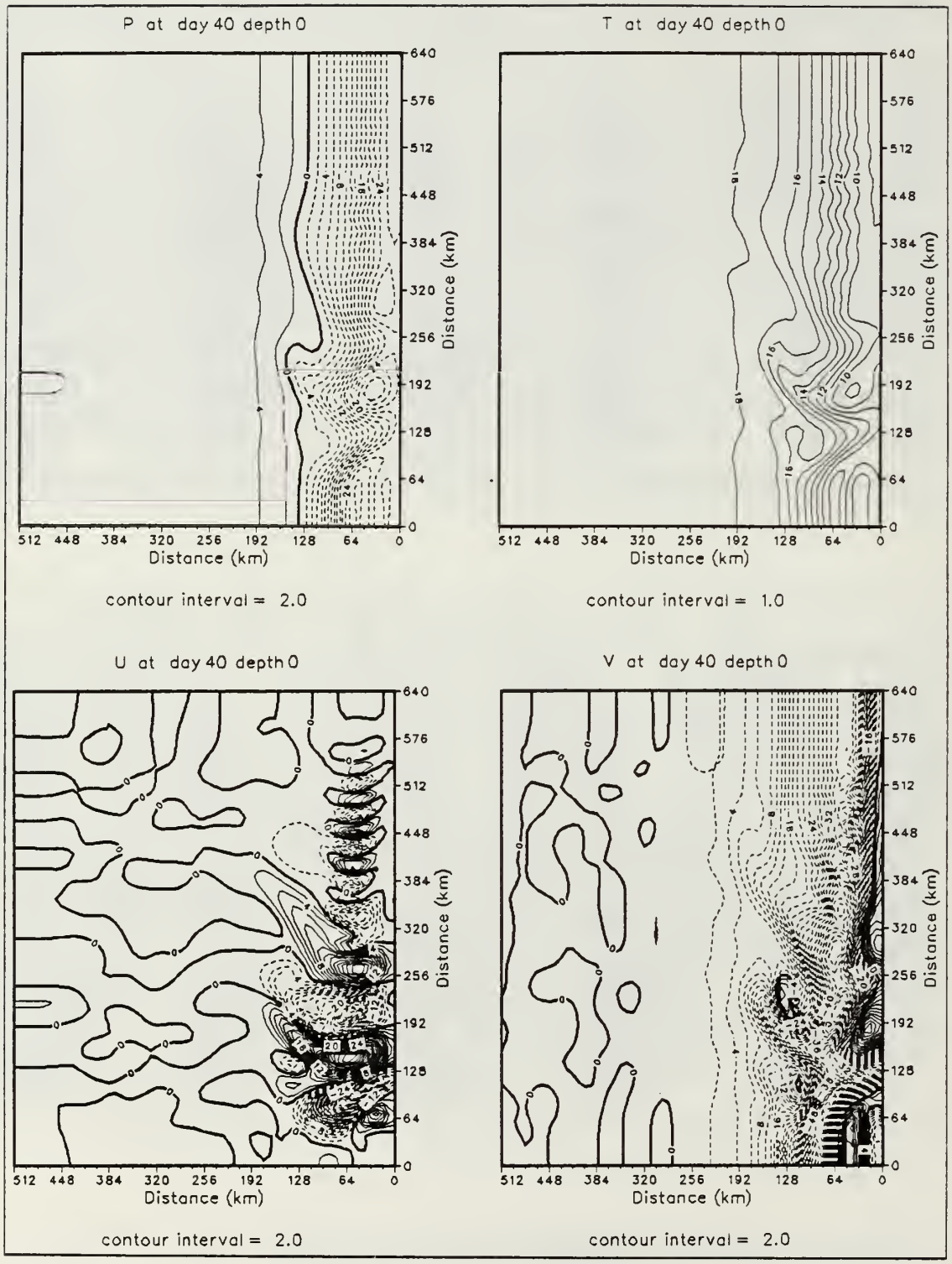

Figure 3.3 Four different fields from Experiment 1 at 40 days.

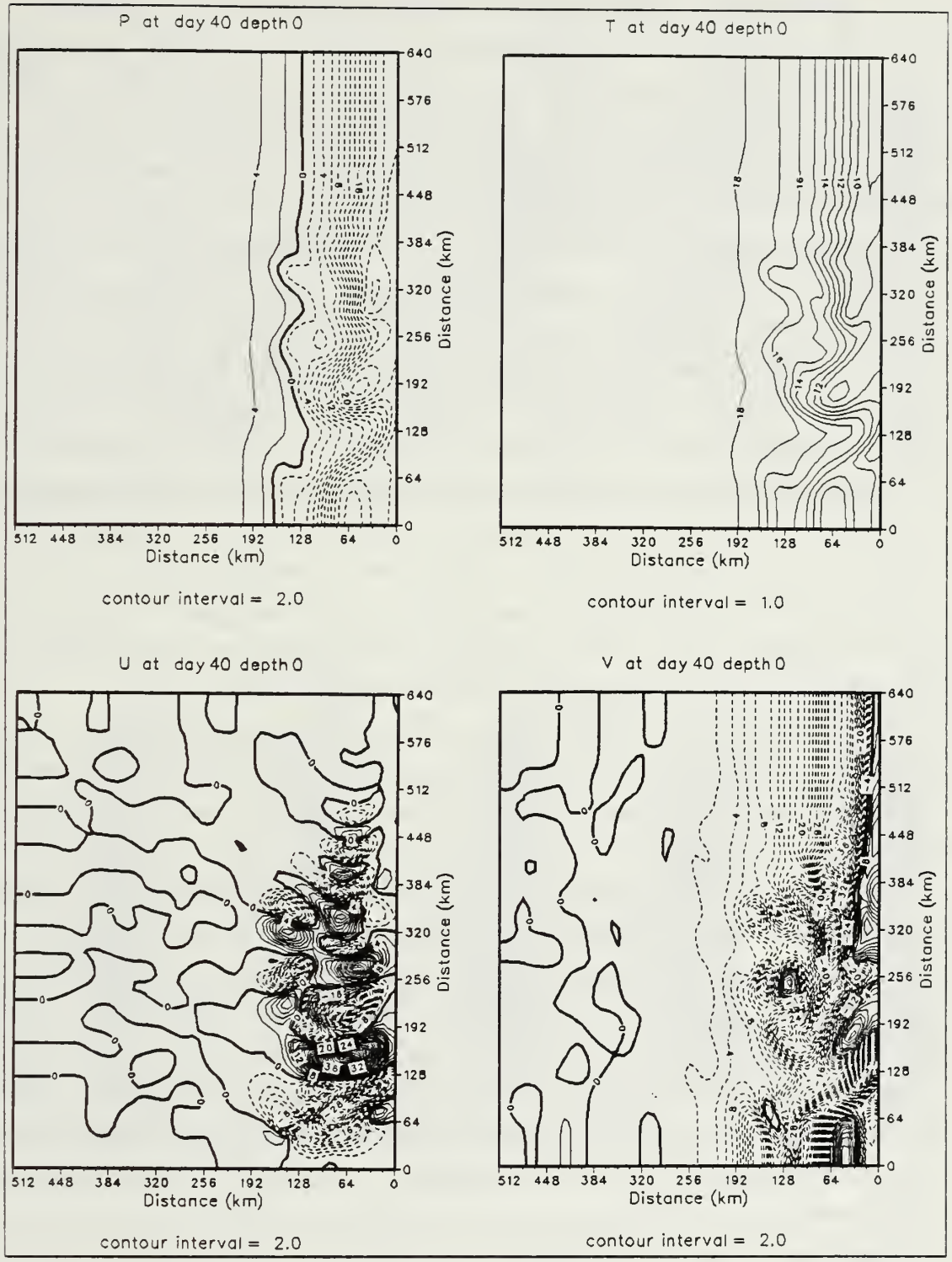

Figure 3.4 Four different fields from the flat bottom case at 40 days.

B. EXPERIMENT 2 (ESCARPMENT SHALLOWEST TO THE NORTH)

By comparison with the actual bottom topography (Fig. 2.2), the escarpment with the shallowest depth to the north (Fig. 2.4) is the most realistic, though still idealized, bottom topography for the California Current region. The width of the escarpment is 60 km and the top of the escarpment is at y = 360 km. This means that the steepest part of the escarpment slope is located in the center of the domain at y = 320 km (or latitude = 39.5∘ as in Fig. 2.4). The depth change due to the escarpment is 1500 m. The experiment was integrated to 40 days. The U-field time series (every 2 days) is shown in Fig. 3.5 and Fig. 3.6. By comparing the surface U-field with Experiment 1, the patterns look similar during the first 10 days, but from 30 days onward a steady flow affected by topography, with symmetry at the center of the escarpment, is developed. The zero velocity is along the center of the escarpment ($\sim$y = 320 km) with off-shore flow (negative U) on the north side of the escarpment and on-shore flow (positive U) on the south side of the escarpment. The in-shore velocity is larger than the off-shore velocity at surface, but at the depth 790 m, the in-shore velocity and the off-shore velocity are the same. This development of a quasi-steady pattern, with no eddies, after 40 days is very different from the previous case (Experiment 1) having only off-shore variation in topography.

Fig. 3.7 shows four different fields at 40 days. The temperature field at the coast is 9 ∘C, and offshore it is 18 ∘C. The temperature increases upstream (north) of the escarpment and downstream (south) of the escarpment with the lowest temperature directly over the escarpment. The surface pressure field shows the geostrophic flow pattern best. The pressure pattern shows a trough over the escarpment with a ridge downstream of it. The isobars are pinched together (as are the isotherms) on the downstream side of the trough indicating a strong jet-like flow toward shore.

From the pressure field, it is possible to determine the effects of the escarpment topography with the flow moving from the shallow water column (on the north) to the deep water column (on the south). It is seen that the flow is stabilized by topography so Experiment 2 after 30 days, looks like steady flow. The topography induces a quasi-steady trough-ridge system over the escarpment. In addition, the time-variable eddies which were present in the pressure pattern of Experiment 1 (Fig. 3.3), no longer exist in this experiment with the escarpment. As shown below, the eddies are apparently stabilized by the strong topographic β-effect which is strongest (largest topographic slopes) in this experiment.

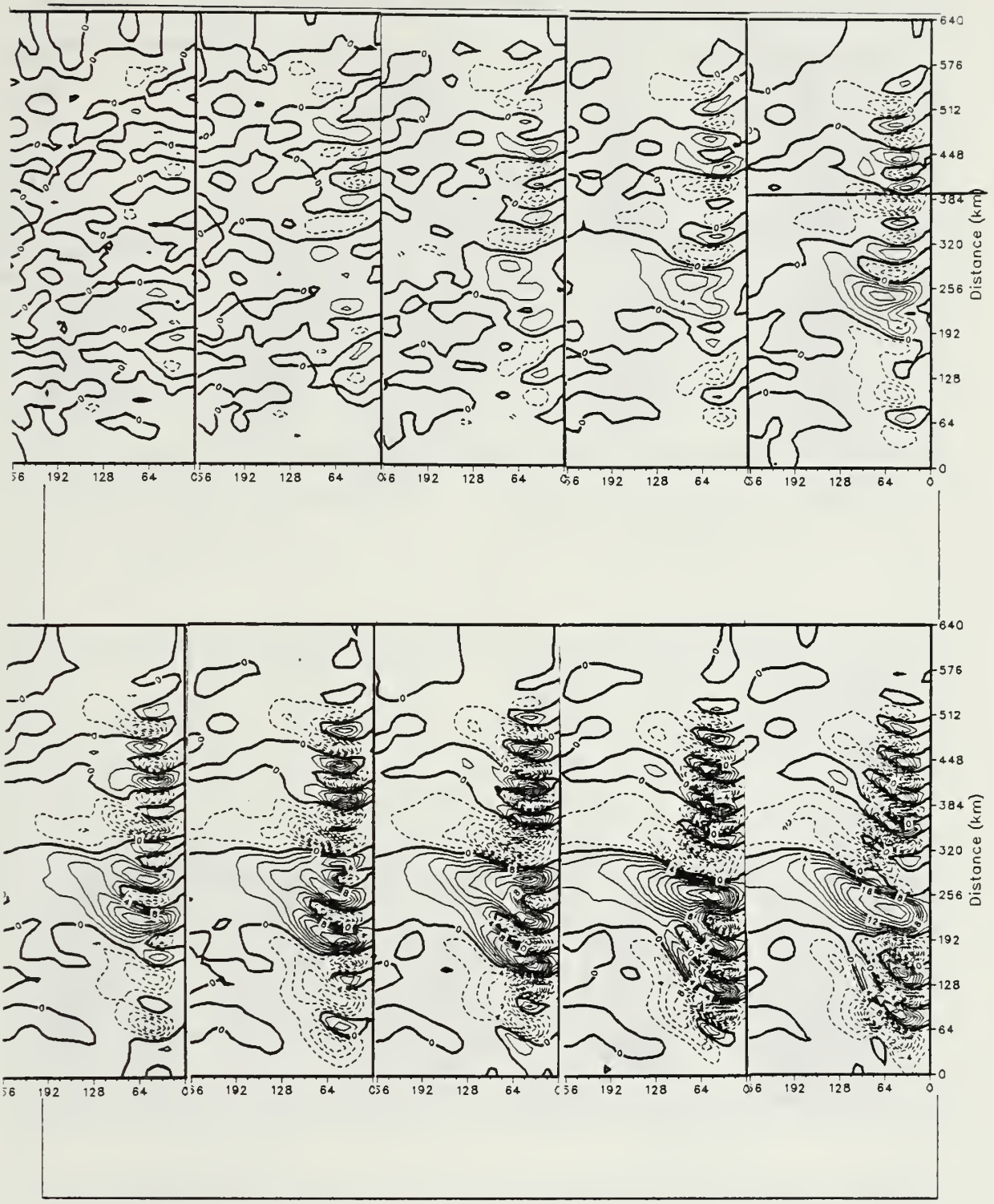

Figure 3.5 The same as Fig. 3.1 except Experiment 2.

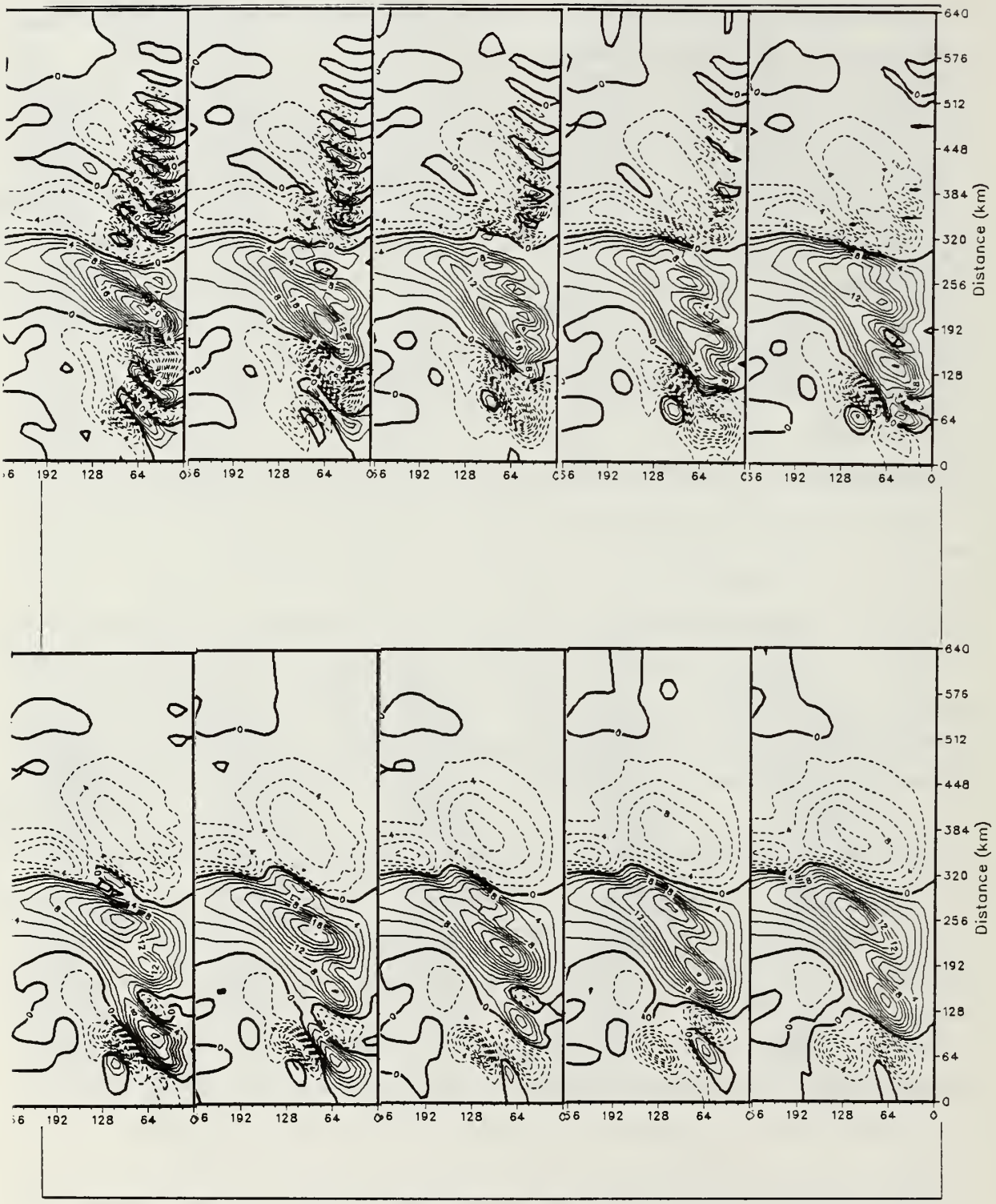

Figure 3.6 The same as Fig. 3.2 except Experiment 2.

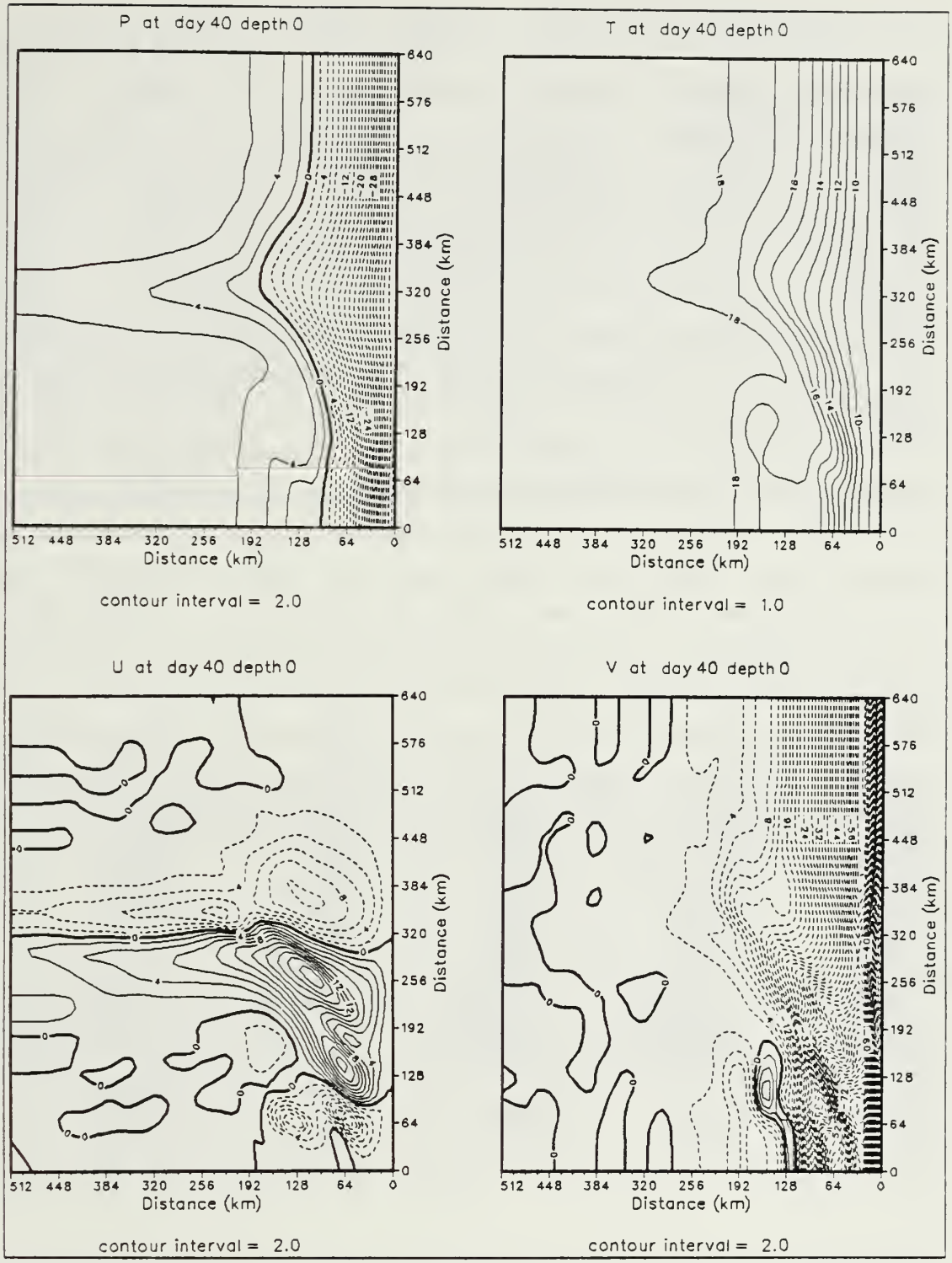

Figure 3.7 Four different fields from Experiment 2 at 40 days.

C. EXPERIMENT 3 (DEEPEST TO THE NORTH)

The escarpment of Experiment 3 (deepest depths to the north) is the reverse of Experiment 2 (shallowest depths to the north). The top of the escarpment is at y = 280km (maximum slope at y = 320 km) and the width of the escarpment and the depth change due to the escarpment are the same as in Experiment 2. This experiment was integrated to day 40. The surface U-field time series (every 2 days) is shown in Fig. 3.8 and Fig. 3.9. The eddies become stronger with time as they propagate southward. There is a large off-shore flow at about y = 280 km. The in-shore flow and off-shore flow is not symmetric across the center of the escarpment.There are only small waves at the north of the escarpment and these waves grow rapidly at the south of the escarpment.

The surface temperature range (not shown) is the same as in Experiment 2. The temperature field is affected by pressure which indicates the geostrophic velocity. The southward surface flow moves from the deep water column to the shallow water column. Particles displaced into shallow water tend to turn to the right in order to acquire anticyclonic vorticity, thus conserving potential vorticity. Although there is a strong tendency for the surface flow to be directed off-shore (U less than zero) over the escarpment, the eddy field is still quite strong at 40 days and the flow is not yet approaching steady state. The results of this experiment are very different from the case with the shallowest depths to the north. Thus, the orientation of the escarpment, whether the shallow water lies to the right or left (looking off-shore), makes a big difference in the flow pattern.

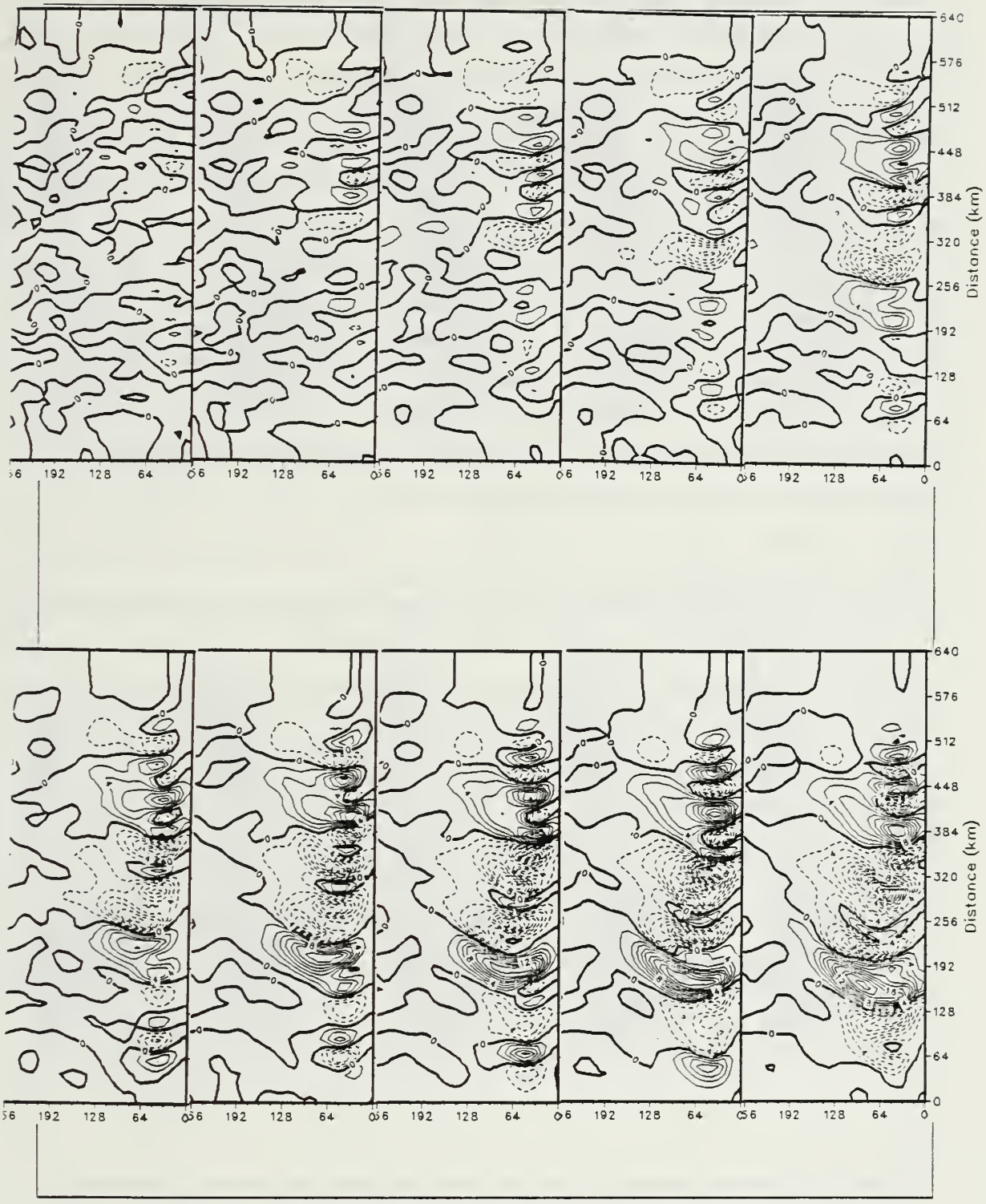

Figure 3.8 The same as Fig. 3.1 except Experiment 3.

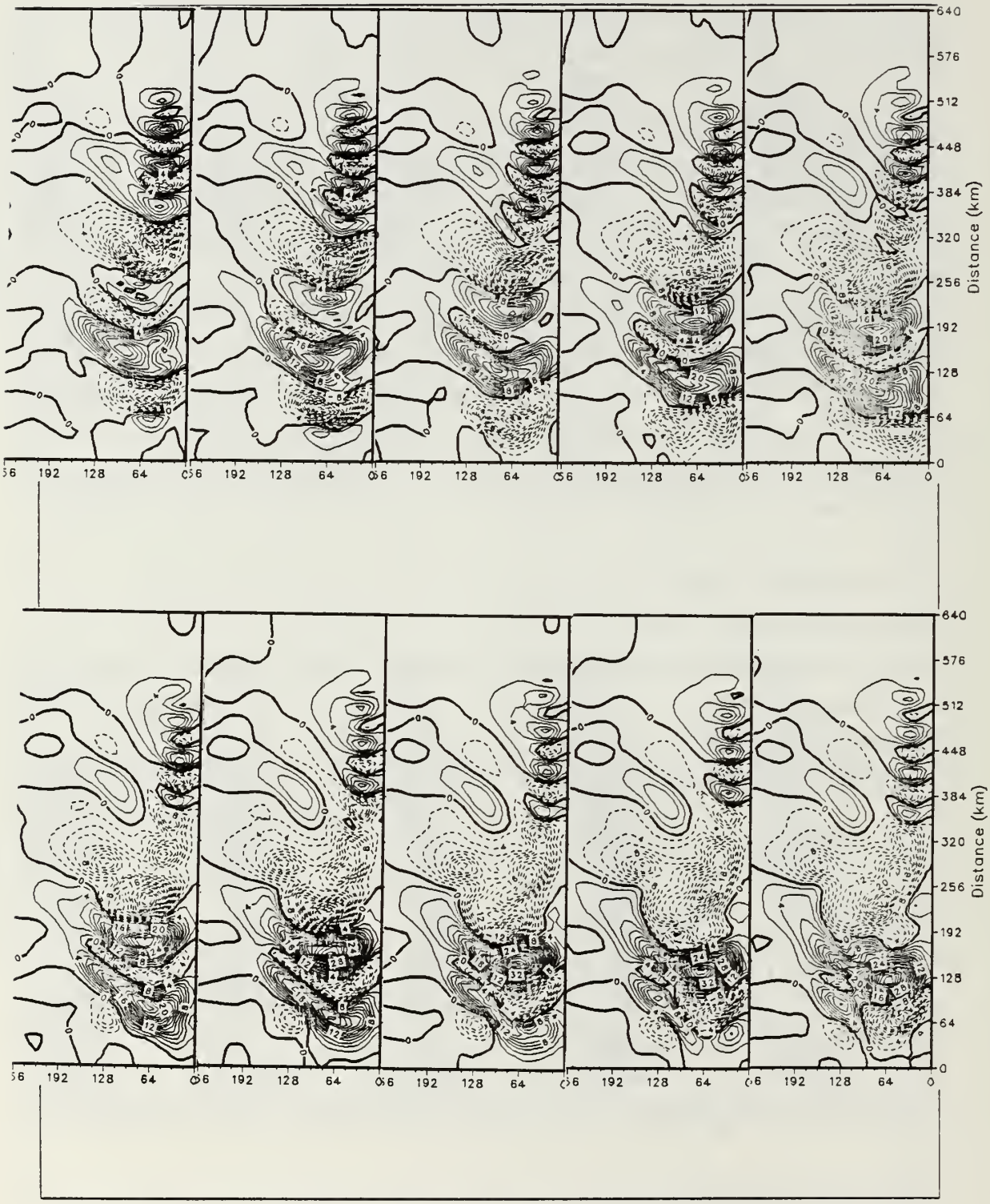

Figure 3.9 The same as Fig. 3.2 except Experiment 3.

D. EXPERIMENT 4 (RIDGE)

Experiment 4 uses a combination of the topographies of Experiment 2 and Experiment 3 to form a topographic ridge (Fig. 2.6). The top of the ridge is in the center of the domain at y = 320 km. The half width of the ridge (Gaussian length scale) is 60 km, so each side of the ridge is exactly the same as the similarly facing escarpment in the previous two experiments. The U-field pattern (Fig. 3.10 and Fig. 3.11) looks like Experiment 2 but the eddies are stronger than Experiment 2. The eddies move to the south and get stronger with time. The in-shore flow downstream from the topographic ridge is larger than the off-shore flow upstream of the topographic ridge. The off-shore flow is over the center of the ridge. This flow is also consistant with the conservation of potential vorticity. Potential vorticity would increase when depth decreases as particles approach the ridge. However particles turn to the right (off-shore) and acquire anticyclonic relative vorticity thus maintaining constant potential vorticity. The reverse happens (particles turn to the left) as the flow goes over the ridge. The result is a trough (positive relative vorticity) over and somewhat downstream of the topographic ridge. From the surface U-field, we can see that this experiment looks like quasi-steady flow after approximately day 30. This result is very similar to the escarpment (only) case with the shallowest water to the north (Experiment 2) but very different from the case with the shallowest water to the south (Experiment 3). It therefore seems that, if the variable bottom topography has a southward facing slope (westward topographic β-effect) as in Experiment 2 and 4, a quasi-steady flow pattern develops. On the other hand, if the topographic β-effect has no westward component (Experiment 1 and 3 and the flat bottom case) then no steady state is reached within 40 days. The four topographic experiments are compared and interpreted in greater detail in the next section.

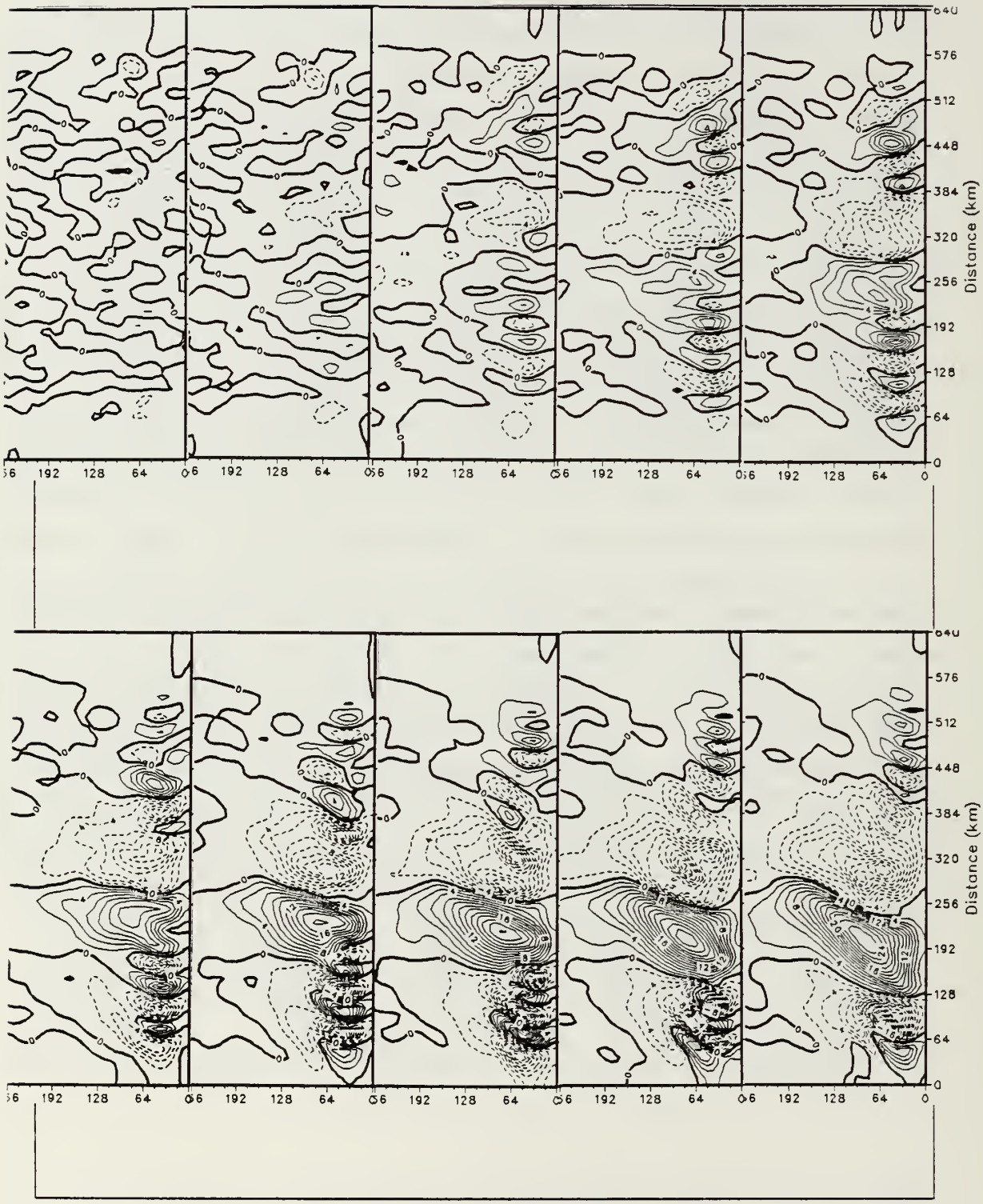

Figure 3.10 The same as Fig. 3.1 except Experiment 4.

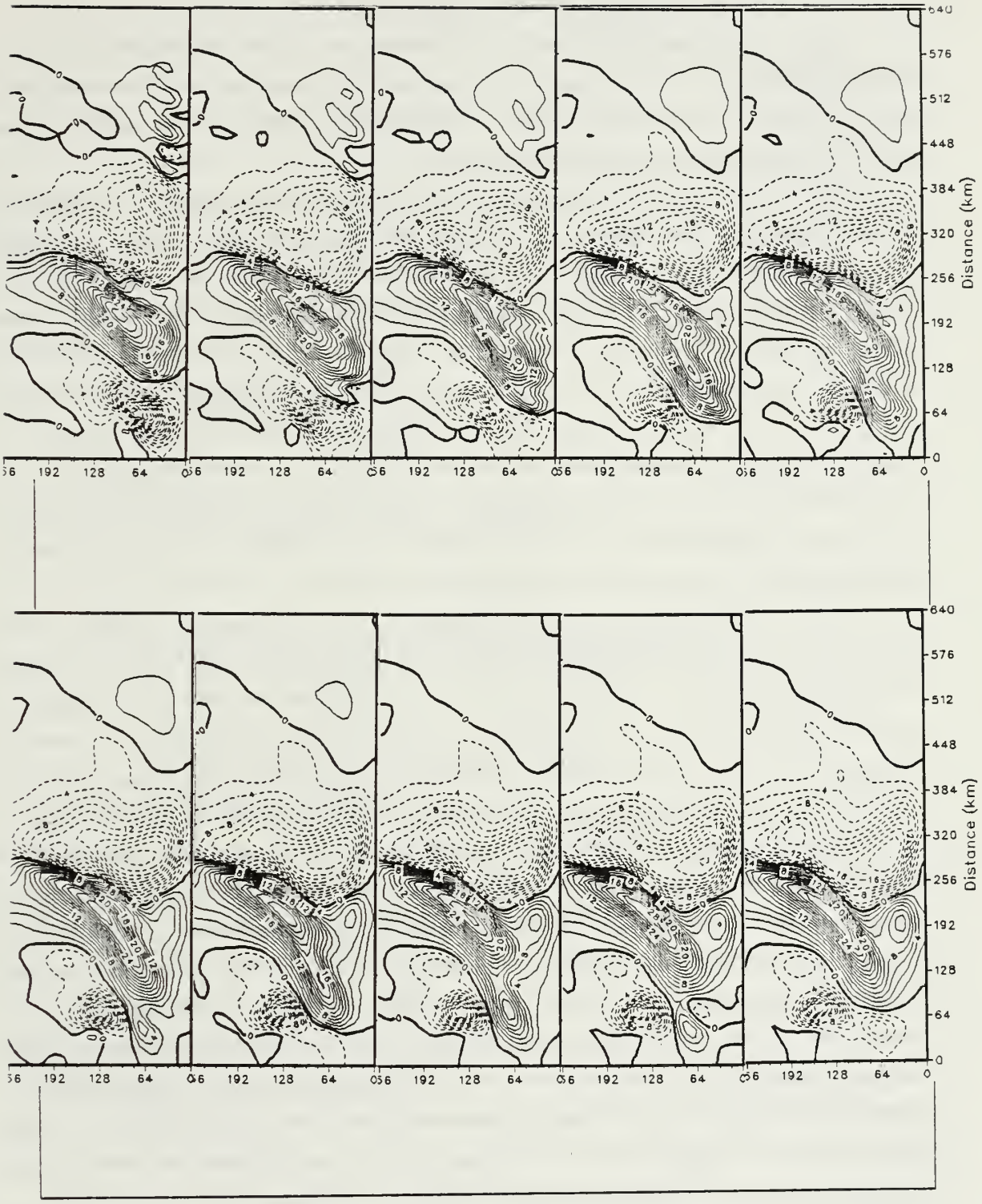

Figure 3.11 The same as Fig. 3.2 except Experiment 4.

E. ANALYSIS AND PHYSICAL INTERPRETATION

The above results can be seen to be characterized by two main features - (1) the establishment (or not) of a quasi-steady response to the topography after 40 days and (2) the growth (or not) of the initial small amplitude random disturbances. In this section we try to interpret these main features.

The four different experiments with variable bottom topography were integrated to day 40 and the four resulting surface pressure fields developed in time series (every ten days) are compared in Figs. 3.12-3.15. The four different fields look much the same at ten days (Fig. 3.12). By comparing the pressure field pattern at day 40, Experiment 3 and Experiment 1 look similar except the amplitude of the main eddy in Experiment 3 (the escarpment deepest to the north) is larger than in Experiment 1 (off-shore slope only). Also, the surface pressure field in Experiment 2 and 4 look the same. The maximum off-shore velocity in Experiment 2 is at the top of the escarpment (y = 360 km) and the maximum off-shore velocity in Experiment 4 is at the top of the ridge (y = 320 km). Experiments 2 and 4 have reached a quasi-steady state but Experiments 1 and 3 have not.

Some of these differences and similarities may be explained in terms of the direction of eddy energy propagation. Due to the topographic β-effect, the eddy energy of the quasi-geostophic, non-dispersive long topographic Rossby waves propagates with the shallow water to the right. The eddy energy in Experiment 1 therefore propagates to the north and that in Experiment 3 propagates along the escarpment in the in-shore direction before turning northward near the coastline. The eddy energy in Experiment 2 propagates along the southward facing escarpment in the off-shore direction, and that in Experiment 4 propagates in the in-shore direction on the north side of the ridge and in the off-shore direction on the south side of the ridge. Thus, there is a mechanism which tends to converge the eddy energy toward the eastern boundary stronger in Experiment 3 than in any of the other experiments. The eddy energy can therefore propagate away, leaving the steady (topographically forced) flow behind, most easily in Experiment 2 and 4 because in both of these cases, and only in these two cases, there is a westward off-shore component to the group velocity vector. This is why the orientation of an escarpment, whether the shallow water is to the right or whether it is on the left when looking off-shore, is important.

We now compare the growth of the initial random disturbances in the different experiments. The flow in Experiment 1 acquires an eddy velocity of 30 cm/sec at about

day 32 and that in Experiment 3 does so at about day 30. The flat bottom case has eddy velocities this big (at about day 22) earlier than Experiment 1 and 3. These differences in the growth of the random disturbances are probably due to the different (stabilizing) effect of the topographic-β in the experiments. We estimate the effects using the simple two-layer model. From Holton, (1981, pages 216-223, two-layer model), we use two parameters β and λ to compute the phase speed and growth rate of the disturbances. The parameter β/h is the mean potential vorticity gradient on an f-plane in the case of a small Rossby number (i.e., topographic-β), and λ is the inverse of the internal Rossby radius of deformation. These two parameters are defind as follows:

$\lambda^2 = f^2_0/(N^2\Delta z^2) \sim$ 2.0 E-13 $1/cm^2$

$\beta = f/h \times \partial h/\partial x \sim$ 2.5 E-12 1/(cmsec) (for experiment 1)

$\beta \sim$ 5.0 E-12 1/(cm.sec) (for experiment 3)

V_m = 20 cm/sec the vertical average meridional wind (upper 720m see Fig.2.7)

V_t = 20 cm/sec the basic state thermal wind (from Fig.2.7)

L_x = 120 km meridional wavelength of eddies

$k = 2\pi/L_x$ = 5.23 E-7 meridional wave number

$C = V_m - \beta(k^2 + \lambda^2)/k^2(k^2 + 2\lambda^2) \pm \sqrt{d}$ phase speed

From Experiment 1 (continental rise) we obtained a phase speed (C_r in Holton) of 11 cm/sec southward and an e-folding time ($1/kC_i$ in Holton) of 2.8 days, and for Experiment 3 we obtained a phase of speed of 2 cm/sec and e-folding time of 3.4 days. From the model results in this study, we estimated the phase speed and growth rate of the eddies from the resulting U-field (Fig.3.1). We obtained a phase speed of 14 cm/sec and growth rate of about 10 days for the Experiment 1 and about the same for Experiment 3. Thus, the random disturbances are baroclinically unstable and grow at about the same rate in both Experiment 1 and 3. By 40 days, the flow in Experiment 3 is in the very early stages of the approach toward a steady state flow over the escarpment (on-shore / off-shore flow). The disturbances appear to be somewhat stronger in Experiment 3 than in Experiment 1, not because of a stronger instability (shorter e-folding time), but rather because of the convergence of Rossby wave eddy

energy at the coast. In Experiments 2 and 4, the topographic β-effect appears to be strong enough, and the direction of eddy energy propagation away from the coast, so these two cases have already reached steady flow by 40 days. The resulting new "mean flow", i.e. the quasi-steady trough / ridge system over and downstream of the escarpment (or ridge) in these experiments, appears to be stable. Future experiments should be aimed at examining the stability of this topographically forced flow to a variety of disturbing effects such as variable winds or boundary forcing.

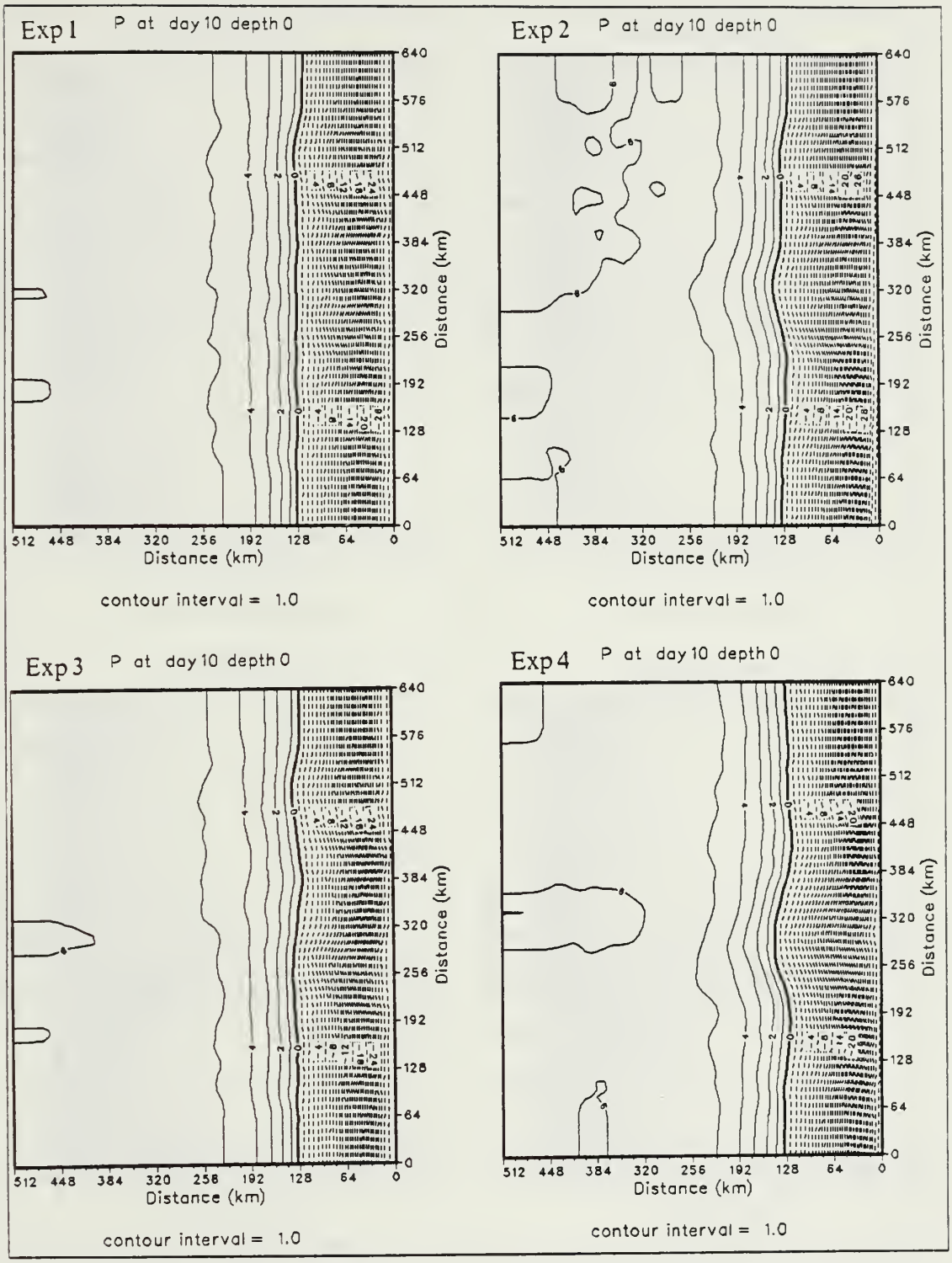

Figure 3.12 Four different pressure fields at day 10.

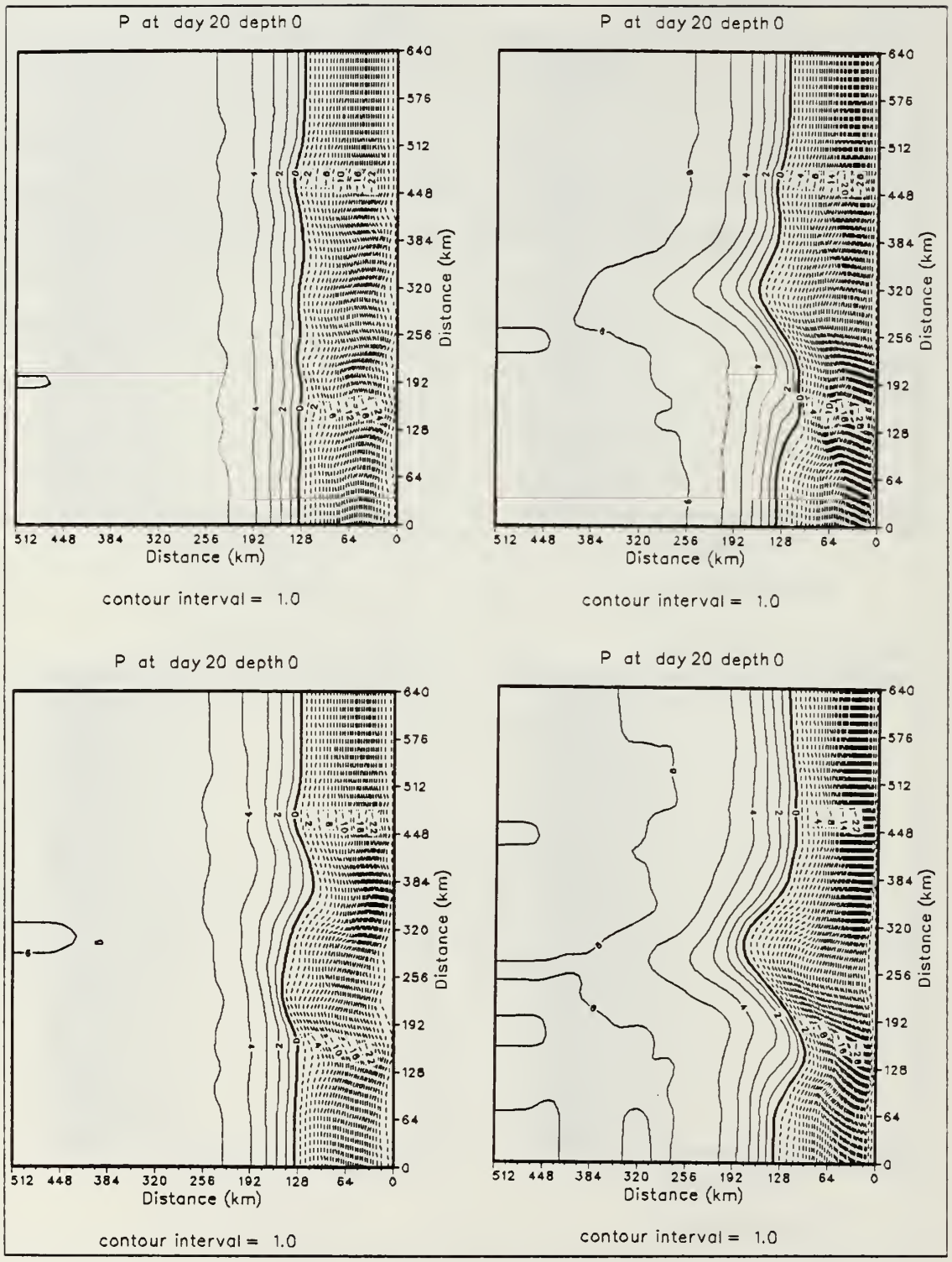

Figure 3.13 Four different pressure fields at day 20.

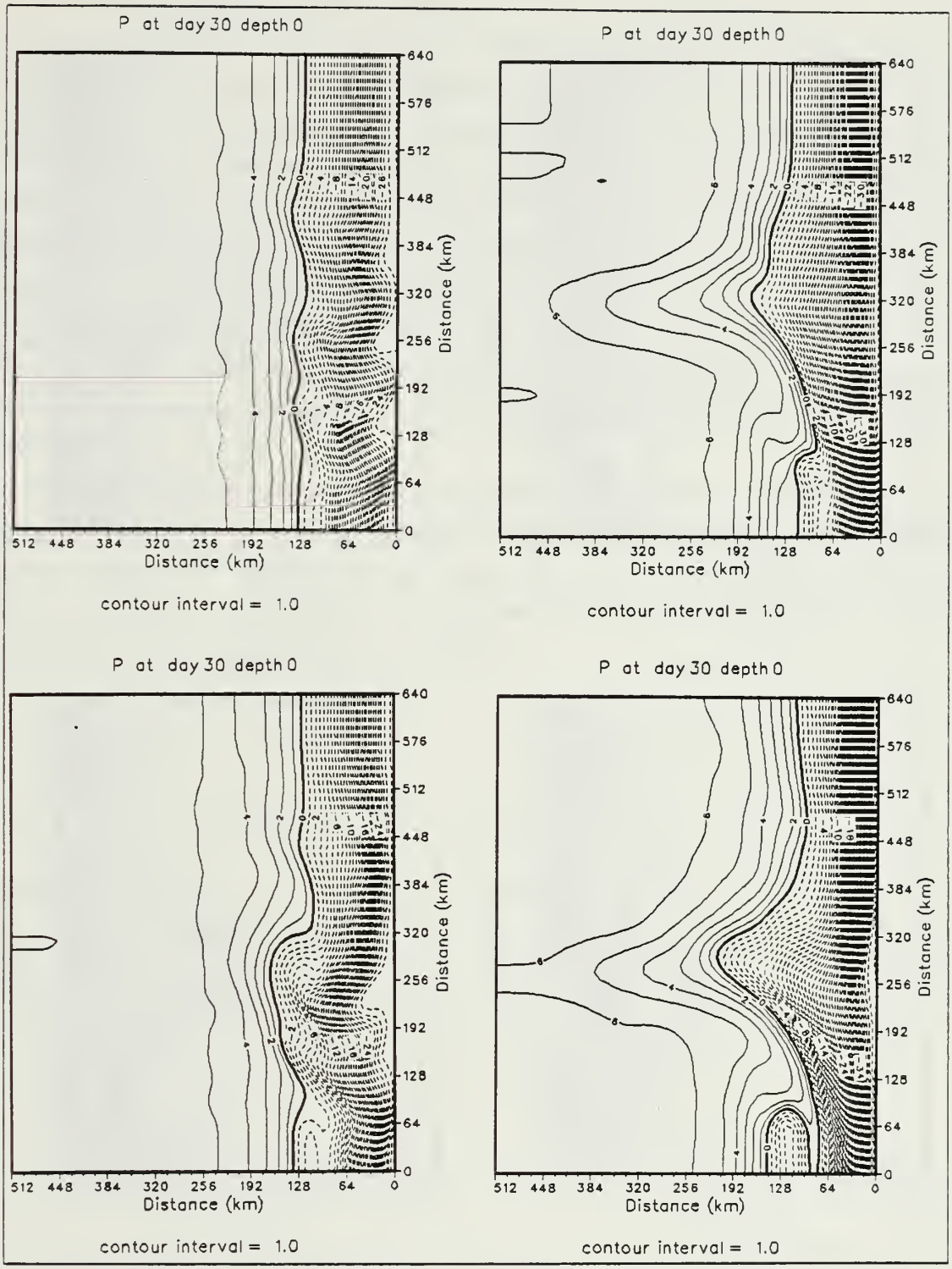

Figure 3.14 Four different pressure fields at day 30.

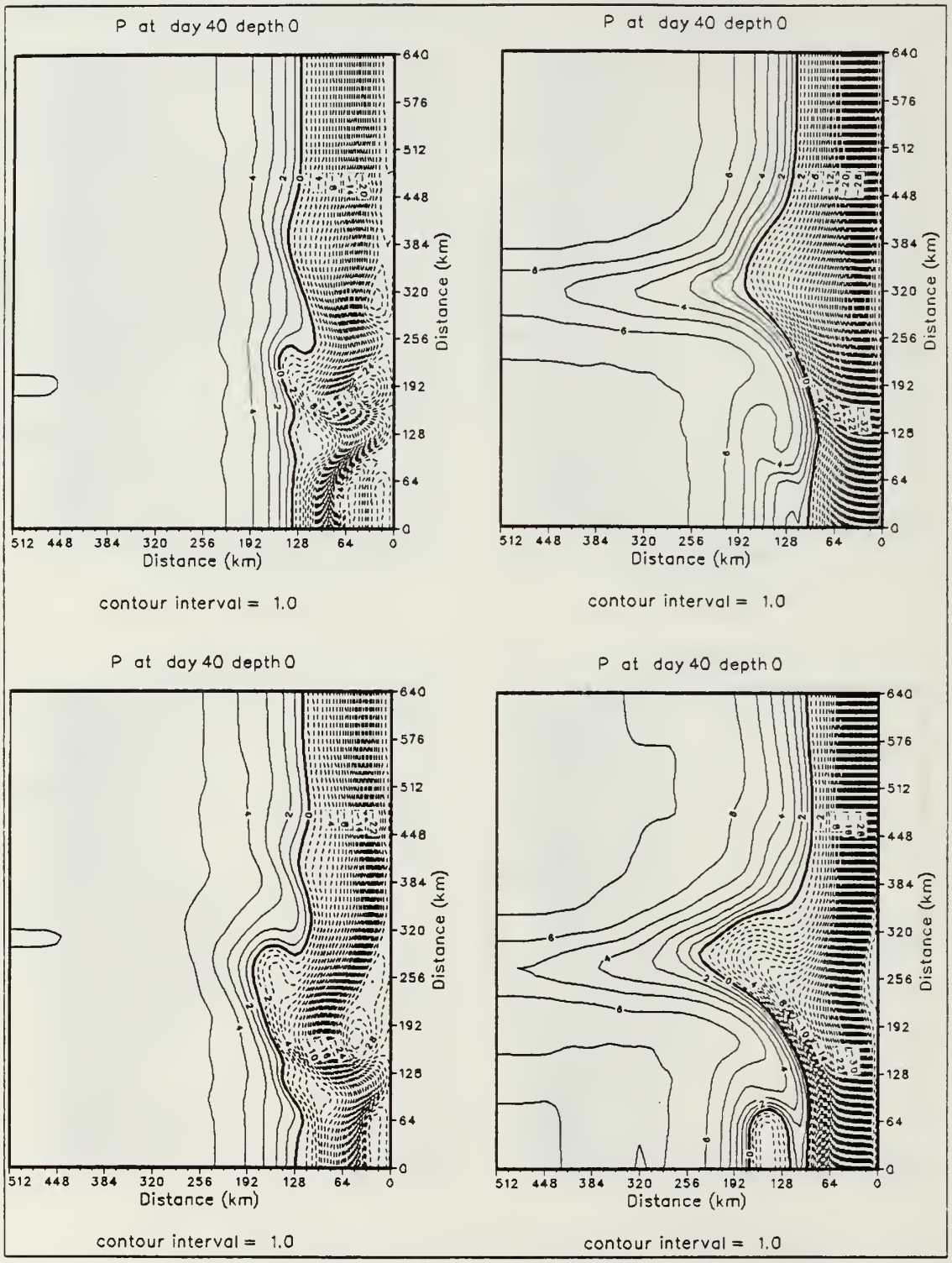

Figure 3.15 Four different pressure fields at day 40.

F. SUMMARY AND CONCLUSION

The objective of this study was to investigate the topographic effects on coastal jet instability. By comparing Experiment 1 and the flat bottom case, we can see the continental rise topography has a stabilizing influence on the mean flow, so the flat bottom case goes unstable approximately ten days earlier than Experiment 1. If the variable bottom topography has a southward facing slope (westward topographic β-effect) as in Experiment 2 and 4, a quasi-steady flow pattern develops. If the topographic β-effect has no westward component as in Experiment 1 and 3, then no steady state is reached within 40 days. From a careful and complete analysis of the analytical and numerical experiments describe above, we conclude that Mendocino Escarpment plays an important role in baroclinic and barotropic instability processes in the CCS.

Since the depth averaged flow was not included in the model used in these experiments, the above studies should be repeated using a model which includes the depth averaged flow. This model could allow the above conclusions to be reevaluated and it would reveal the role of the depth averaged flow, and its interaction with the baroclinic flow and topography in the CCS.

LIST OF REFERENCES

Camerlengo, A. L. and J. J. O'Brien, 1980: Open boundary conditions in rotating fluids. *J. Comput. Physics.*, **35,** 12-35.

Charney, J. G. and G. R. Flierl, 1981: Oceanic analogues of atmospheric motions. In *Evolution of Physical Oceanography*, B. Warren and C. Wunch, Ed., MIT Press, 623 pp.

Emery, W. J. and L. A. Mysak,1980: Dynamical interpretations of satellite-sensed thermal features off Vancouver Island. *J. Phys. Oceanogr.*, **10,** 961-970.

Freitag, H. P. and D. Halpern, 1981: Hydrographic observations off Northern California during May 1977. *J. Geophys. Res.*, **86,** 4248-4252.

Haney, R. L., 1985: Midlatitude sea surface temperature anomalies: A numerical hindcast. *J. Phys. Oceanogr.*, **15,** 787-799.

Holton, J. R., 1981: An introduction to dynamic meteorology. ACADEMIC Press, 391 PP.

Ikeda, M. and W. J. Emery, 1984: Satellite observations and modeling of meanders in the California Current System off Oregon and Northern California. *J. Phys. Oceanogr.*, **14,** 1434-1450.

Killworth, P. D. 1980: Barotropic and baroclinic instability in rotating stratified fluids. *Dynamics of Atmospheres and Oceans.*, **4,** 143-184.

Kosro, P. M. and A. Huyer, 1986: CTD and velocity surveys of seaward jets off Northern California, July 1981 and 1982. *J. Geophys. Res.*, **91,** 7680-7690.

Narimousa, S. and T. Maxworthy, 1985: Two-layer model of shear driven coastal upwelling in presence of bottom topography. *J. Fluid Mechanics.*, **159,** 503-531.

Orlanski, I. and M. D. Cox, 1973: Baroclinic instability in ocean currents. *Geophysical Fluid Dynamics.*, **4,** 297-332.

Peffley, M. B. and J. J. O'Brien, 1976: A three-dimensional simulation of coastal upwelling off Oregon. *J. Phys. Oceanogr.*, **6,** 164-180.

Preller, R. and J. J. O'Brien, 1980: The influence of bottom topography on upwelling off Peru. *J. Phys. Oceanogr.*, **10,** 1377-1398.

Thomson, R. E., 1984: A cyclonic eddy over the continental margin of Vancouver Island: Evidence for baroclinic instability. *J. Phys. Oceanogr.*, **14,** 1326-1348.

Wright, D. G., 1980: On the stability of a fluid with specialized density stratification. Part 2. Mixed baroclinic-barotropic instability with application to the northeast Pacific. *J. Phys. Oceanogr.*, **10,** 1307-1322.

INITIAL DISTRIBUTION LIST

		No. Copies
1.	Defense Technical Information Center Cameron Station Alexandria, VA 22304-6145	2
2.	Library, Code 0142 Naval Postgraduate School Monterey, CA 93943-5002	2
3.	Chairman, Department of Oceanography Code 68 Naval Postgraduate School Monterey, CA 93943-5000	1
4.	Chen, Ching-Yin No. 2, Lane 68, Sec. 1, Chung-Shan Rd., Wu-Fu, Yung-Ching, Chang-Hwa Hsien, Taiwan, Republic of China	5
5.	Professor R. L. Haney Code 63HY Department of Meteorology, Naval Postgraduate School Monterey, CA 93943	2
6.	Professor R. T. Williams Code 63WU Department of Meteorology, Naval Postgraduate School Monterey, CA 93943	1
7.	Real Admiral Yao, Neng Chun Chinese Naval Hydrographic and Oceanographic Office Tsoying, Kaohsiung Taiwan 813 Republic of China	1
8.	Kuo, Feng-Yu Chinese Naval Hydrographic & Oceanographic Office Tsoying, Kaohsiung Taiwan 813 Republic of China	1
9.	Professor Mary Batteen Code 68BN Department of Oceanography, Naval Postgraduate School Monterey, CA 93943	1
10.	Professor David Smith Code 68SM Department of Oceanography, Naval Postgraduate School Monterey, CA 93943	1
11.	Chen, Kuei-Ying No. 16, Lane 70, Yu-Feng St., Ku-Shan Ch'u, Kaohsiung, Taiwan, Republic of China	2

220969

Thesis
C4105
c.1

Chen
Topographic influence
in the California Current
System.